HHS Public Access

Author manuscript

Neurobiol Aging. Author manuscript; available in PMC 2022 December 31.

Published in final edited form as:

Neurobiol Aging. 2022 December ; 120: 149–166. doi:10.1016/j.neurobiolaging.2022.08.006.

Behavioral and fMRI evidence that arousal enhances bottom-up selectivity in young but not older adults

Sara N. Gallant[1], **Briana L. Kennedy**[2], **Shelby L. Bachman**[1], **Ringo Huang**[3], **Christine Cho**[1], **Tae-Ho Lee**[4], **Mara Mather, PhD**[1]

[1]Davis School of Gerontology, University of Southern California, Los Angeles, CA

[2]School of Psychological Science, University of Western Australia, Perth, Australia

[3]Department of Psychology, University of California, Los Angeles, Los Angeles, CA

[4]Department of Psychology, Virginia Tech, Blacksburg, VA, United States

Abstract

The locus coeruleus-noradrenergic system integrates signals about arousal states throughout the brain and helps coordinate cognitive selectivity. However, age-related changes in this system may impact how arousal coordinates selectivity in older adults. To examine this, we compared how increases in emotional arousal modulates cognitive selectivity for images differing in perceptual salience in young and older adults. Using functional magnetic resonance imaging, we found that relative to older adults, hearing an arousing sound enhanced young adults' bottom-up processing and incidental memory for high versus low salience category-selective body images. We also examined how arousing sounds impacted a top-down goal to detect dot-probes that appeared immediately after high or low salience images. We found that young adults were slower to detect probes appearing after high salience body images on arousing trials, whereas older adults showed this pattern on non-arousing trials. Taken together, our findings show that arousal's effect on selectivity changes with age and differs across bottom-up and top-down processing.

Corresponding Author: Mara Mather, PhD, Professor, School of Gerontology, University of Southern, California, 3715 McClintock Ave, Los Angeles, CA, USA 90089, mara.mather@usc.edu.

Disclosure Statement

The authors have no conflicts of interest to declare.

Data Statement

Behavioral data will be available at https://osf.io/4276j/ and MRI data at OpenNeuro.org.

CRediT Author Statement

Sara Gallant: Conceptualization, Methodology, Software, Formal Analysis, Investigation, Writing – Original Draft, Visualization, Project Administration, Funding Acquisition.
Briana Kennedy: Software, Investigation, Writing - Review & Editing, Project Administration.
Shelby Bachman: Formal Analysis, Writing – Original Draft, Writing – Reviewing & Editing.
Ringo Huang: Software, Formal Analysis, Writing – Reviewing & Editing.
Christine Cho: Project Administration, Formal Analysis.
Tae-Ho Lee: Writing – Reviewing & Editing.
Mara Mather: Supervision, Conceptualization, Methodology, Writing – Reviewing & Editing.

Submission Declaration and Verification

We confirm that this work has not been published previously and is not under consideration for publication elsewhere. All authors have approved the manuscript submission in its current form.

Keywords

arousal; selectivity; bottom-up; top-down; memory; aging; neuroimaging

1. Introduction

Increases in arousal help selectively tune attention to relevant aspects of our environment (Mather & Sutherland, 2011). This adaptive response can be triggered by spikes in arousal associated with a threat to survival or more common events like hearing a jarring sound, completing an effortful task, or experiencing certain emotions. The locus coeruleus (LC), the brain's primary source of noradrenaline (NA), integrates signals about arousal states in the brain via its broad efferent network (Aston-Jones & Cohen, 2005; Samuels & Szabadi, 2008). LC neurons have both tonic and phasic modes of activity. The tonic mode is characterized by elevated baseline LC activity with low levels of phasic LC firing. The phasic mode is characterized by moderate baseline LC activity with high levels of phasic LC firing. During the phasic mode, excitation of highly active neurons and suppression of less active neurons is enhanced (Sara, 2009; Sara & Bouret, 2012). This is thought to facilitate cognitive selectivity during an arousing event, when LC phasic activity is high, resulting in enhanced attention for high salience information (Clewett et al., 2018; Jacobs et al., 2020; Lee et al., 2018, 2013).

The glutamate amplifies noradrenergic effects (GANE) theory outlines how arousal-induced NA released from the LC can bias perceptual processing and memory formation in favor of high over low priority information (Mather et al., 2016). Priority is determined by a top-down goal or differences in bottom-up salience. The GANE model posits that, at cortical sites of prioritized representations, enhanced levels of glutamate (an excitatory neurotransmitter) interact with local NA to create hotspots of excitation. At the same time, cortical sites associated with weaker representations without NA hotspots are suppressed. According to GANE, these interactions between the LC-NA system and local cortical activation contribute to arousal-enhanced selectivity of high over low priority mental representations, which then in turn should affect later memory for these representations.

The GANE model also argues that NA's influence on neural gain under arousal manifests at the whole-brain level (Mather et al., 2016). Frontoparietal regions are thought to coordinate selective processing of prioritized cortical representations under arousal due to their role in encoding the priority of information (Ptak, 2012). These regions are also highly innervated by NA neurons and are stimulated by LC-NA activation (Samuels & Szabadi, 2008). Phasic LC responses modulate activity in a dorsal frontoparietal network, which guides detection of goal-relevant stimuli (Corbetta et al., 2008; Lee et al., 2018; Sara & Bouret, 2012). NA also enhances activity in a ventral attention network, which guides attention based on external factors such as perceptual salience. This ventral network includes the ventral frontal cortex and temporoparietal junction (TPJ), lateralized to the right hemisphere (Bowling et al., 2020; Corbetta & Shulman, 2002; Shomstein, 2012). NA projections from the LC are thought to underlie the TPJ's bottom-up attention-orienting function (Corbetta et al., 2008). For instance, propranolol, a beta-adrenergic blocker, blunts TPJ responses to novel stimuli

(Strange & Dolan, 2007) and TPJ lesions are associated with reduced P3 event-related potential responses (Nieuwenhuis et al., 2005) that tracks phasic NA activity (Vazey et al., 2018). Thus, LC-NA projections to frontoparietal regions likely play a role in coordinating attention selectivity under arousal.

Recent work testing the GANE model has found arousal is more effective at enhancing perceptual processing for high over low priority information in young than in older adults (Durbin et al., 2018; Gallant et al., 2020; Lee et al., 2018). In a study by Lee and colleagues (2018), a tone conditioned to predict shock (CS+) was used to increase arousal on a trial-by-trial basis while young and older adults detected the location of a high-priority image that was both perceptually salient and goal-relevant. When compared to a tone that did not predict shock (CS−), the CS+ selectively increased young adults' brain activity for high over low salience images. Older adults showed no increase in selectivity under arousal as the CS+ increased their brain activity for both high and low salience images. This age difference in arousal-induced selectivity was linked to age differences in the interaction between the LC and frontoparietal brain regions. When comparing age groups, the authors found that the CS+ increased functional connectivity of the LC and dorsal frontoparietal regions when detecting high salience images in young but not in older adults. Thus, increases in arousal were deemed less effective at coordinating selective processing in older adults. This is consistent with predictions from the GANE model about how aging should impact the effect of arousal on selectivity based on age-related changes in the LC-NA system such as loss of LC neurons (Mather et al., 2016).

However, in Lee and colleagues (2018) study, bottom-up and top-down influences on arousal-induced selectivity could not be dissociated. In their task, the priority of high salience images was determined by bottom-up and top-down factors as they were both perceptually salient and goal-relevant (participants' goal was to indicate the location of high salience images). This previous work also exclusively concerned the impact of arousal on perceptual processing, and so it is not clear how arousal influences subsequent memory selectivity based on salience. In the current study, we sought to address these unanswered questions concerning age differences in arousal-induced selectivity in attention and memory: How does arousal impact selectivity in bottom-up processing and incidental memory of high over low salience images? How does arousal modulate top-down detection of goal-relevant stimuli?

To address these questions, we modified Lee et al.'s (2018) task by separating the presentation of high and low salience images from the top-down detection task. Emotional arousal was manipulated on a trial-by-trial basis using negative or neutral sound clips. We defined bottom-up selectivity as biases driven by image salience. Given that perceptual contrast is considered a primary route to bottom-up priority (Mather & Sutherland, 2011) and a primitive saliency component (Itti & Koch, 2000), we manipulated bottom-up salience via perceptual contrast. Bottom-up selectivity was indexed by comparing brain activity and incidental memory for category-selective images differing in salience. Category-selective images of bodies and scenes that activate specialized brain regions, including the extrastriate body area (Downing et al., 2001) and parahippocampal place area (Epstein & Kanwisher, 1998) respectively, were used to isolate arousal's effect on mental representations in

localized cortical regions. We also compared activity for high and low salience images in the right TPJ, a node of the ventral attention network involved in bottom-up orienting that receives input from the LC-NA system (Corbetta et al., 2008). Based on the GANE model, we expected arousal to be more effective at increasing selectivity in young relative to older adults (Mather et al., 2016). For young adults, we predicted that arousal would enhance category-selective brain activity, right TPJ activity, and incidental memory for high versus low salience images. In contrast, for older adults, we did not expect arousal to amplify bottom-up selectivity.

We also examined arousal's impact on a top-down goal to detect probes that appeared in the location of a high or low salience image. We hypothesized that arousal may facilitate reaction times (RT) to detect probes in the location of high salience images in young adults. This was based on Lee et al.'s (2018) finding of arousal-enhanced neural selectivity when young adults detected the locations of high versus low salience images. However, as described earlier, high salience images in that study were not just salient but also goal-relevant, so whether those results reflect bottom-up or top-down processes cannot be disentangled. In other work, arousal has shown to strengthen bottom-up selectivity (Lee et al., 2013; Sutherland & Mather, 2012; Sutherland et al., 2017) but weaken top-down attention in young adults (Pessoa, 2009; Sutherland et al., 2017). Given these latter findings, it is also possible that arousal could slow RTs to detect probes in the location of high salience images.

Finally, we tested potential LC-NA system contributions to age differences in arousal-induced selectivity by measuring LC structure and function. We used a turbo-spin echo (TSE) MRI protocol (Sasaki et al., 2006) that enables LC delineation and used a semi-automated procedure to estimate contrast ratios from these images as a measure of LC structure (Liu et al., 2017). Consistent with work using this LC structure measure in distinct age groups, we expected age differences in LC contrast ratios (Clewett et al., 2016; Liu et al., 2017). LC function was estimated from ROI analysis of BOLD signal and pupil size in response to the arousal manipulation as pupil dilation has been linked to LC function (Murphy et al., 2014). In general, we expected to see greater LC ROI and pupil responses to our arousal manipulation (Clewett et al., 2018; Jacobs et al., 2020). As it is unknown whether these measures of LC structure and function covary with outcomes associated with LC-NA processes, we conducted exploratory analyses to probe the relationship between LC contrast ratios, LC BOLD activity, and behavioral and fMRI outcomes.

2. Material and Methods

2.1 Participants

Participants were invited to participate if they met certain inclusion criteria as assessed via self-report during recruitment. Invited participants were right-handed, had no history of psychiatric or neurological disorders, were not taking beta-blocker medications, had normal or corrected-to-normal vision (via prescription eyeglasses or contacts), had normal hearing (i.e., did not use hearing aids and had no diagnosed or self-reported hearing impairments). The final sample included 30 young adults aged 19–29 years (M = 23.43, SD = 2.83) and 30 older adults aged 60–85 years (M = 70.63, SD = 6.16). All participants received

$75 USD for their participation. Three participants' data were excluded and replaced: One young adult because of an incidental finding in their MRI images, one older adult because the MRI-compatible response pad malfunctioned, and one older adult whose data were not saved to the MRI scanner due to a technical issue.

Table 1 displays characteristics of the final sample. There were no group differences in education or the ratio of males to females. On the 21-item Depression Anxiety Stress Scales (DASS-21; (Lovibond & Lovibond, 1995), scores fell in the normal range with no significant age differences in depression or stress, but higher levels of anxiety in young than in older adults. Older adults also scored higher than young adults on the Shipley Vocabulary Test (Shipley, 1940). Participants were screened for cognitive impairment using the Montreal Cognitive Assessment (MoCA; (Nasreddine et al., 2005). Scores were in the normal cognition range (>26) for both groups.

2.2 Materials

2.2.1 Category-selective stimuli.—Stimuli included neutral images of bodies and scenes to activate the EBA (Downing et al., 2001) and the PPA (Epstein & Kanwisher, 1998), respectively. For the incidental encoding task, 96 clothed body images (including 32 full body, 32 torso only, 32 legs only) and 96 scene images (48 indoor, 48 outdoor) were selected from previous studies (Downing et al., 2006; Kaiser et al., 2014; Orlov et al., 2010; Taylor et al., 2007), the SUN database (Xiao et al., 2010), and the Internet[1]. This resulted in a total of 192 images within each stimulus category. Each body and scene image was yoked with an image from the same category that was perceptually different (e.g., two pictures of a torso wearing shorts or two pictures of a kitchen), which served as a lure during the recognition task. Which of these images was old or new during the memory task was counterbalanced across participants. An additional novel 36 body images and 36 scene images was selected for a functional localizer task that was used to delineate the EBA and PPA. Images were resized to 300×300 pixels and normalized to the mean luminance of all images using the SHINE toolbox in MATLAB (Willenbockel et al., 2010).

During the incidental encoding task, half of the images appeared as high salience and the remaining half appeared as low salience, with an equal proportion of body and scene images in each salience condition. The bottom-up salience of images was manipulated using an approach like Lee et al. (2018) by presenting one of the two images in full contrast, making it more visually salient than the other low contrast image. The perceptual contrast of half of the images was degraded by 80% to create low salience images. A yellow border was applied to the remaining images to create high salience images. Image salience was counterbalanced, such that all images were equally in the high or low salience condition.

2.2.2 Sound clips.—Sound clips were used to induce arousal on a trial-by-trial basis. A set of 48 negative arousing and 48 neutral non-arousing 6-second sound clips were selected

[1]To confirm that bodies and scenes did not differ in arousal at baseline, we collected ratings of arousal using an online survey (N = 20). Participants viewed images included in the study and were asked to rate the image on a scale of 1 (not at all arousing) to 5 (very arousing). The results indicated that body and scene images did not differ in average arousal level (M = 2.24 and 2.03 respectively, t = 0.95, p = .34).

from the International Affective Digitized Sounds database (Bradley & Lang, 2007). Sounds were selected based on valence and arousal norms provided by the dataset. Examples of negative arousing sounds include gunshots, a car accident, a woman screaming, a person vomiting, a couple fighting. Examples of neutral non-arousing sound clips include animal sounds, people talking, typing on a keyboard, a toilet flushing, a lawnmower, or brushing teeth. After selecting sound clips, Audacity® recording and editing software (version 2.4.2; https://audacityteam.org/) was used to trim sound clips to include the most intense 3 seconds of each clip. Given that sound clips were altered, we collected additional ratings from participants using a 5-point Likert-style self-assessment manikin ranging from 1 = not arousing at all to 5 = very arousing.

2.2.3 Incidental memory task.—The experimental tasks were programmed in MATLAB Psychophysics Toolbox Version 3. Figure 1 shows a sample trial from the incidental encoding task. Participants first heard a sound clip while fixating on a cross at the center of the screen. A body and scene image pair then appeared side by side, one with high salience and the other with low salience. The location of images on the left or right side of the screen was randomized for every participant. After a 500 ms interstimulus interval (ISI), a dot probe appeared in the location of either the high or low salience image (there were an equal number of high and low salience probes). Participants detected the probe location as quickly as possible by pressing a button with their index (left response) or middle finger (right response) on a fiber optic fMRI-compatible response pad held in their right hand. During the encoding task, there were a total of 96 body-scene image pairs displayed.

Memory for all images seen during incidental encoding was tested on a surprise recognition memory task outside of the scanner. On each trial, a pair of images from the same stimulus category was presented (e.g., two body images or two scene images) and participants indicated if they had seen it during encoding (see Figure 1). There were 224 trials, including 192 old trials and 32 new trials. Half of the old trials consisted of 96 body image pairs that included the old body image yoked with a categorically similar lure. The remaining half of the old trials consisted of 96 scene image pairs yoked with a categorically similar lure. The 32 new trials consisted only of lure images from the same category (16 body image pairs and 16 scene image pairs) to garner an estimate of guessing (i.e., false alarms).

On each trial of the recognition memory task, participants were presented with a body image pair or a scene image pair and selected which image was old or if they were both new. There were three possible responses: to indicate the left image was old, to indicate the right image was old, or to indicate that both images were new. Responses were self-paced and were made using the keyboard by pressing keys labeled as ‘L’ for left, ‘R’ for right, and ‘New’. The location of images on the left or right side of the screen was randomized for every participant and images were counterbalanced as old or new.

2.2.4 Functional localizer task.—A functional localizer task was designed to localize body and scene selective voxels in the brain. The task had a blocked design, including three body and three scene blocks of 14 trials each. Each trial started with a fixation cross for 500 ms followed by a single image (a body or scene, depending on the block) that was presented for 150 ms. To parallel the design of the incidental encoding task, the image in each trial

appeared either on the left or right side of the screen. Within each block, two of the images were repeated in sequence. To keep participants engaged, they were asked to press a button on the response pad whenever they saw a repeated image. Responses were made using the right index finger and were only required on repeated trials. A similar approach has previously been used to identify category-selective regions (Johnson et al., 2007; Wojciulik et al., 1998; Yi & Chun, 2005).

2.3 Procedure

All procedures adhered to guidelines for ethical human subject research as approved by the Institutional Review Board at University of Southern California. Participants provided informed consent prior to starting the experiment. This was followed by the DASS-21, Shipley Vocabulary Test, and a background questionnaire, all administered using Qualtrics survey platform. The experimenter then conducted the MoCA. After this and before entering the scanner, 12 practice trials for the incidental encoding task were completed (Figure 1). Participants were told that, after hearing a sound, two images would flash on the screen, then a dot would appear in the location of one of the images. They were instructed to view the images as we were measuring how the brain responded to different image types and that their primary task was to detect the location of the dot as quickly as possible. Participants were unaware that their memory for images would be tested later.

The scanning protocol lasted approximately one hour. The high-resolution T1-weighted MPRAGE anatomical scan was acquired first followed by a T1-weighted TSE scan, which was used to delineate the LC in the brainstem. After structural scans, fMRI volumes were collected across three blocks of the incidental encoding task (Figure 1), which each consisted of 32 trials. Sounds were played through Sensimetrics Model S14 MRI-compatible earbuds. Between each block, participants were reminded of the task instructions and to keep their head as still as possible. The incidental encoding task took ~18 min to complete. The functional localizer task followed the incidental encoding task and consisted of six blocks (3 bodies, 3 scenes) of 14 trials, each separated by 8 seconds. The task lasted approximately ~1.5 minutes. The scanning session concluded with a 5-min resting state scan, the results of which are not included here.

Once outside of the scanner, participants completed the self-paced surprise recognition task (128 trials) for old images from the incidental encoding task mixed with new lure images. Following the recognition task, the 96 sound clips were rated on arousal level. Pupil dilation was continuously measured during the rating task using a Gazepoint GP3 60 Hz research-grade portable eye tracker. Participants fixated on a blank screen while listening to a sound clip for 3 s after which they made a self-paced arousal judgment. Responses were made via mouse click using a 5-point self-assessment manikin ranging from 1 (not arousing at all) to 5 (very arousing).

2.4 MRI Data Acquisition

Neuroimaging data were acquired on a 3T Siemens Magnetom Prisma MRI system in the Center for Image Acquisition at USC Keck School of Medicine. Stimuli were displayed on a 32-inch Cambridge Research BOLDscreen 32 with a 1980×1080 pixel widescreen LCD

display and a fixed 120 Hz frame rate, viewed via a mirror attached to a 32-channel matrix head coil. A high-resolution T1-weighted MPRAGE anatomical sequence was acquired first to help with functional image co-registration and LC delineation (TR = 2300 ms, TE = 2.26 ms, TI = 1060 ms, 176 interleaved slices, flip angle = 9°, FoV = 256mm, slice thickness = 1mm with no gap, bandwidth = 200 Hz/Px, GRAPPA acceleration factor = 2, 1mm isotropic voxel size). This was followed by a two-dimensional, multi-slice T1-weighted turbo-spin echo (TSE) sequence (TR = 750 ms, TE = 10 ms, 11 axial slices, flip angle = 120°, FoV = 220mm, bandwidth = 287 Hz/Px, slice thickness = 2.5mm, slice gap = 1.0 mm, in-plane resolution = 0.429mm^2), which helped to visualize the LC as a hyperintense region adjacent to the floor of the fourth ventricle (Sasaki et al., 2006). Functional images for the localizer task (111 volumes) and three blocks of the encoding task (170 volumes each) were acquired using a multiband echoplanar sequence (TR = 2000 ms, TE = 54.60 ms, 88 interleaved slices with no gaps, flip angle = 52°, FoV = 222mm, bandwidth = 2228 Hz/Px, acceleration factor = 8, and 1.7mm isotropic voxel size).

2.5 Behavioral and Pupil Analyses

2.5.1 Subjective arousal ratings and pupil dilation response to sound clips.

—We first examined the effect of sound type on subjective arousal ratings and pupil dilation during the rating task. To determine the effect of sound type on subjective arousal level, each participant's ratings were averaged and analyzed in a 2 (age group: young, older) × 2 (arousal: arousing, non-arousing) mixed-effects ANOVA.

The pupillometry data were preprocessed using MATLAB (Mathworks, MA). Blinks and other artifacts were removed from the signal using a semi-automated program developed in our lab (github.com/EmotionCognitionLab/ET-remove-artifacts). The program detects blinks using an algorithm based on the velocity profile of each participants' pupil time course (Mathôt et al., 2013) and linearly interpolates over the detected blink region. Time courses were manually corrected when the presence of non-blink artifacts impeded the precision of the blink-removal algorithm. Segments of non-blink artifacts that exceeded a duration of 1 s were classified as missing data and ignored in analyses.

For the pupil dilation analysis, we computed baseline pupil diameter and change in pupil diameter for each sound. If over half of the samples from a single trial were imputed with missing data indicators, then the trial was removed from analyses. After applying these exclusion criteria, the data from 25 older adults and 29 young adults were included in the pupil analysis. Average pupil dilation was examined in response to arousing and non-arousing sounds. To determine dilation over each trial, we subtracted the average pupil diameter during the 500 ms period before sound onset from the average pupil diameter during the 3 second period after sound onset. These baseline normed pupil dilation responses were analyzed in a 2 (age group: young, older) × 2 (arousal: arousing, non-arousing) mixed-effects ANOVA.

We also examined correspondence between subjective and objective markers of arousal across age groups, specifically whether trial-by-trial pupil dilations predicted subjective ratings across arousal levels and age groups. Linear mixed-effect models (LMM) were used to model the data, implemented in R using the lme4 (Bates et al., 2015) and lmerTest

(Kuznetsova et al., 2017) packages. Subjective ratings were the dependent variable and arousal condition (coded as 1 = arousing, 0 = non-arousing), age group (coded as 1 = young, −1 = older), and continuous sound-evoked pupil dilation were modeled as fixed effects. Participant intercepts were modeled as random effects (i.e., random variance in intercepts due to unexplained differences between participants (Meteyard & Davies, 2020).

2.5.2 Attentional bias scores.—Arousal-induced selectivity was inferred by greater processing of high salience versus low salience stimuli on arousing trials within each stimulus category. Given that bodies and scenes belong to distinct stimulus categories with distinct cortical representations (Downing et al., 2001; Epstein & Kanwisher, 1998), we included stimulus type as a factor in our models to determine if age differences in arousal-induced selectivity differed for bodies and scenes.

We examined reaction times (RTs) to detect dot-probes during the incidental encoding task as a function of age group, arousal level of the trial, and if the dot-probe appeared in the location of a high or low salience image. Prior to analysis, RTs from error trials were removed so that only correct responses were analyzed. We also trimmed trials with RTs that were 2.5 SDs above or below each participant's mean RT prior to computing mean RTs for each condition. Trimmed means were then used to calculate attention bias scores for each arousal and stimulus condition with a previously used formula (Mather & Carstensen, 2003):

$$attention\ bias\ score\ =\ mean\ low\ salience\ probe\ RT\ -\ mean\ high\ salience\ probe\ RT$$

where low salience probe RT reflects responses to probes in the location of low salience images and high salience probe RT reflects responses to probes in the location of high salience images. Positive attention bias scores thus indicate a bias to attend to high salience images and negative scores indicate a bias to attend to low salience images. Attention bias scores were analyzed in a 2 (age group: older, young) × 2 (arousal: arousing, non-arousing) × 2 (stimulus type: bodies, scenes) mixed-effects ANOVA and one-sample t-tests to determine whether age groups were more or less likely to attend to high or low salience images on arousing and non-arousing trials.

2.5.3 Recognition memory analyses.

As described earlier, on old trials of the recognition task, an old image was paired with a categorically similar lure (Figure 1). This made for three possible recognition outcomes: hit, gist hit, or miss. Hits occurred when the participant indicated the correct image was old. Gist hits occurred when the participant indicated the categorically similar lure was old. We refer to them as gist hits because these responses suggest that the participant recognized the image category but was unable to discern which of the two images was old. Misses occurred when the participant indicated both images were new.

Analysis of recognition memory performance focused primarily on hit and false alarm rates. To determine age differences in arousal-induced memory selectivity, hit rates were submitted to a 2 (age group: older, young) × 2 (arousal: arousing, non-arousing) × 2 (salience: high salience, low salience) × 2 (stimulus type: bodies, scenes) mixed-effects ANOVA. We also

examined age differences in false alarm rates in a 2 (age group: young, older) × 2 (stimulus type: bodies, scenes) ANOVA. Finally, we computed an index of recognition discrimination accuracy (hits minus false alarms; (Snodgrass & Corwin, 1988) as a measure of participants' ability to distinguish old from new items. Discrimination accuracy was computed as a function of age group and stimulus type (body and scene) since it was not possible to calculate separate false alarm rates according to levels of arousal or salience, which were only varied during encoding and not recognition. Discrimination accuracy scores were analyzed in a 2 (age group: young, older) × 2 (stimulus type: bodies, scenes) ANOVA.

2.6 Neuroimaging Preprocessing and Analysis

Image preprocessing was carried out with FMRIB Software Library (FSL, www.fmrib.ox.ac.uk/fsl). Functional volumes were processed using FSL's FMRI Expert Analysis Tool (FEAT, Version 6) with the following steps: motion correction using MCFLIRT, non-brain tissue removal using BET, spatial smoothing using a Gaussian kernel of 5mm full-width-at-half-maximum, grand-mean intensity normalization of the entire 4D dataset by a single multiplicative factor, and high-pass temporal filtering (Gaussian-weighted least-squares straight line fitting, with sigma = 50.0s). Independent component analysis (ICA) was carried out using MELODIC to identify unexpected artifacts or activation (Beckmann & Smith, 2004). To classify noise components, FMRIB's ICA-based Xnoisefier (FIX) auto-classifier was run on single-subject ICA outputs. The FIX classifier was trained on 10 single-subject ICA datasets from the current study in which noise artifacts related to head motion, white matter/CSF signal, cardiac or respiratory pulsation, artery activation, or the multiband MRI-sequence were manually identified and removed (Griffanti et al., 2017). The auto-classifier then classified noise components from the remaining 50 single-subject ICA datasets.

For whole-brain analysis, each participant's denoised mean functional volume was registered to their T1-weighted anatomical image using boundary-based registration (BBR) with FSL's FLIRT (Jenkinson et al., 2002). An affine transformation with 12 degrees of freedom was then used to register anatomical images to MNI-152 standard-space with 2mm resolution.

After FSL image preprocessing and ICA denoising, manual quality checks were performed. For each functional run for each participant, we ensured that the relative motion was no more than half a voxel and that absolute motion was no more than one voxel. None of the participants exceeded this cut-off. In addition, before removal of noise components from functional data, the components identified by FIX auto-classifier were manually examined to ensure proper noise classification according to the guidelines described in Griffanti et al. (2017).

2.6.1 Whole-brain voxel-wise analysis.—

For the incidental encoding task, a general linear model (GLM) was set up to examine processing of high versus low salience category-selective images on arousing compared to non-arousing trials. Event-related time vectors were created that modeled the onset times of the image pairs, with a duration of 600 ms, and were used as task regressors in the model. A lower-level GLM was built for each participant

using four task regressors: (1) arousing high salience body and low salience scene, (2) arousing low salience body and high salience scene, (3) non-arousing high salience body and low salience scene, and (4) non-arousing low salience body and high salience scene. Each regressor was convolved with the canonical hemodynamic response function (HRF). Contrasts were created to test for main effects of arousal (arousing minus non-arousing), salience (high minus low salience), and arousal-by-salience interactions (arousing high salience minus arousing low salience, non-arousing high salience minus non-arousing low salience). A second lower-level GLM was conducted that modeled the onset times of the sound clips to better isolate the effects of arousal on LC function and its association with LC contrast and pupil dilation. Contrasts in this analysis tested for main effects of arousal (arousing minus neutral trials). Second-level fixed-effects analyses were then conducted to average each participant's functional runs for the incidental encoding task. The contrast images from the second-level analyses were then analyzed in a group-level random-effects analysis computed with fMRIB's mixed-effects FLAME 1 model (Beckmann et al., 2003; Beckmann & Smith, 2004; Damoiseaux et al., 2008). Clusters were determined by thresholding statistical images at Z > 2.3, corrected with a family-wise error rate ($p < .05$) at the cluster level.

For the localizer task, a lower-level GLM was designed to determine active voxels associated with viewing body images versus scene images and vice versa. For this analysis, we modeled the onset times of images with a duration of 150 ms. The lower-level GLM included two task regressors, one for bodies and one for scenes, which were convolved with canonical HRF. Contrasts compared activation for bodies relative to scenes and for scenes relative to bodies using an uncorrected voxel-based threshold of $Z = 2.3$.

2.6.2 Regions of interest (ROI) analysis.—ROI analyses were performed to determine age differences in the interaction of arousal and salience in the EBA and PPA. These ROI masks were individually defined based on significant clusters of activation that were identified in the lower-level GLM analysis of the functional localizer task. The EBA and PPA ROIs were defined as 6-mm radius spheres that were centered on the peak voxel that was most selective for bodies (bodies > scenes contrast; $Z = 2.3$, uncorrected) and for scenes (scenes > bodies contrast; $Z = 2.3$, uncorrected), respectively. ROIs were localized for all participants for the EBA (mean peak voxel MNI coordinates: left hemisphere [−48 −78 2]; right hemisphere [54 −68 −4]) and PPA (mean peak voxel MNI coordinates: left hemisphere [−22 −42 −12]; right hemisphere [20 −34 −16]). This approach to defining category-selective ROIs has been previously used (Downing et al., 2006) and allowed us to equate the approximate number of voxels within each mask and ensure regions were defined objectively.

Using Featquery in FSL, EBA and PPA masks were aligned to each participant's statistical parametric maps from the second-level GLM analysis that modeled the onset times of images during the incidental encoding task and percent signal change values were calculated. To test our hypothesis that arousal would selectively enhance activation in body- and scene-selective voxels in young but not older adults, we performed separate 2 (age group: young, older) × 2 (arousal: arousing, non-arousing) × 2 (salience: high salience,

low salience) × 2 (hemisphere: left, right) × 2 (stimulus type: bodies, scenes) mixed-effects ANOVAs on the extracted percent signal change means from each ROI.

We also examined age differences in the arousal-by-salience interaction in the right TPJ, a node of the ventral attention network involved in salience-driven attention (Kahnt & Tobler, 2013). We focused on the right TPJ given evidence the ventral attention network is lateralized to the right hemisphere (Fox et al., 2006). The TPJ mask was created using a connectivity-based parcellation atlas (Mars et al., 2012), which includes anterior and posterior TPJ subdivisions in the right hemisphere. These clusters were combined and binarized using fslmaths in FSL. The final mask extended from MNI coordinates [68 −31 22] to [60 −61 22]. Percent signal change within this mask during incidental encoding was then calculated using featquery. The resulting means were extracted and analyzed in a 2 (age group: young, older) × 2 (arousal: arousing, non-arousing) × 2 (salience: high salience, low salience) mixed-effects ANOVA.

Finally, we examined the effect of arousal on LC activity. To create an LC mask, we used a mask in 0.5mm MNI152 standard space from a previous study (Keren et al., 2009). To warp the mask, we first co-registered the 0.5mm linear brain to MNI152 2mm standard space using the “antsRegistrationSyN.sh” routine in Advanced Normalization Tools (ANTS) v2.3.4 (Avants et al., 2009). The resulting transformations were then applied to warp the LC mask into 2mm space. The warped mask was then applied to statistical parametric maps from the second-level GLM that modeled the onset times of sound clips during the incidental encoding task and percent signal change in the LC was calculated with featquery. The extracted means were submitted to a 2 (age group: young, older) × 2 (arousal: arousing, non-arousing) mixed-effects ANOVA.

2.6.3 Calculation of LC contrast ratios.—An automated approach was used to delineate the LC on TSE scans. This entailed bringing participants’ TSE scans into MNI-ICBM 152 0.5 mm linear space using routines within ANTS v. 2.3.4 (Avants et al., 2009). A previously validated approach was used (Dahl et al., 2019), detailed in the Supplementary Methods.

Using the TSE template generated during LC delineation (warped to MNI 0.5mm linear space), we confirmed that at a group level, TSE hyperintensities fell within the LC map (Keren et al., 2009) used for functional analyses (Figure 2). We applied this LC mask on individual TSE scans in MNI 0.5mm linear space to isolate probable LC voxels for contrast ratio calculation. In line with the anatomical boundaries of the LC, we restricted the search for probable LC voxels to MNI z = 85 to 112 (Ye et al., 2021). For each participant, the intensity of the peak voxel across all z-slices within the masked region was extracted for each hemisphere separately. We then masked each participant’s TSE scan in MNI 0.5mm linear space with a publicly available 4×4mm reference region covering the central pontine region (Dahl et al., 2020) and extracted the peak intensity value across all z-slices in the masked region. LC contrast ratios were calculated from peak intensities as follows (Liu et al., 2017):

$$LC\ contrast = \frac{peak(LC) - peak(reference)}{peak(reference)}$$

Resulting LC ratios were analyzed in a 2 (age group: young, older) × 2 (hemisphere: left, right) mixed-effects ANOVA. One participant was excluded from this analysis because a susceptibility artifact was overlapping the pons in their TSE scan. To validate this automated approach, we used a manual protocol for assessing LC intensity (Liu et al., 2017). We calculated the consistency of resulting LC peak intensities across methods via two-way mixed intraclass correlation coefficients (ICC), which are reported in the Supplementary Results.

2.6.4 Associations between LC function, LC contrast, and pupil dilation.—

Finally, we used Pearson's correlation analyses to probe relationships between LC contrast, LC function, pupil dilation, and behavior in each age group. To examine relationships with behavior, a selectivity index was computed as recognition of high salience images minus recognition of low salience images separately for arousing and non-arousing trials. Fisher's *r*-to-*z* transformations were used to compare correlation coefficients between age groups.

3. Results

3.1 Behavioral and Pupillometry Results

3.1.2 Subjective arousal ratings and pupillary responses to sounds.—

As expected, subjective arousal ratings were higher for arousing (M = 3.82, SD = .95) than non-arousing sounds (M = .73, SD = .24), $F(1, 57) = 572.86$, $p < .001$, $\eta_p^2 = .91$, and older adults showed overall higher ratings than young adults (M_{older} = 2.42, SD = .33 vs. M_{young} = 2.14, SD = .52), $F(1, 57) = 5.72$, $p = .02$, $\eta_p^2 = .09$. A significant interaction between age group and arousal, $F(1, 57) = 7.04$, $p = .01$, $\eta_p^2 = .11$, on subjective ratings further showed arousing sounds were rated as higher in arousal by older adults (M = 4.14, SD = .75) than by young adults (M = 3.52, SD = 1.04), $p = .01$, 95% CI [−1.089, −.144]. There was no age difference in ratings for non-arousing sounds (young: M = .77, SD = .23, older M = .69, SD = .25), $p = .26$, 95% CI [−.054, .195]. Similarly, consistent with our hypothesis, pupil responses were greater for arousing than non-arousing sounds, $F(1, 52) = 56.36$, $p < .001$, $\eta_p^2 = .52$, but there were no other significant effects or interactions on pupil responses, $Fs \leq 2.55$, $ps \geq .12$.

The LMM analyses queried the relationship between age group, pupil dilation, and sound type on arousal ratings (Table 2). Mirroring the ANOVA results on ratings, there was a main effect of arousal as well as a significant interaction of age group and arousal showing that older adults' ratings were higher than young adults for arousing sounds (Figure 3A). There was also an interaction of arousal and pupil dilation on ratings. Plotting this interaction showed that pupil dilation to arousing sounds were more positively associated with subjective ratings, β = 137.75, 95% CI [13.07, 262.44], $t = 2.17$, $p = .03$, than pupil dilation to non-arousing sounds, β = 3.09, 95% CI [−78.44, 140.22], $t = 0.55$, $p = .58$ (Figure 3B). Together, these findings suggest that the arousal manipulation had a similar effect on

young and older adults as both groups showed greater subjective ratings and pupil responses to arousing vs. non arousing sounds.

3.1.3 Attention bias scores.[2]

The ANOVA on attention bias scores showed an age × arousal × stimulus type interaction, $F(1, 59) = 7.57$, $p = .008$, $\eta_p^2 = .11$. The age × arousal interaction was significant for body images, $F(1,59) = 5.75$, $p = .020$, $\eta_p^2 = .09$, but not for scene images, $F = 3.09$, $p = .09$. For young adults, a one-sample *t*-test showed a negative attention bias score for body images ($M = -.017$, $SD = .04$) on arousing trials, $t(29) = -2.60$, $p = .014$, $d = -0.43$, whereas there was no evidence of an attention bias on non-arousing trials, $t = -.73$, $p = .47$. This indicates that, on arousing trials, young adults were quicker to detect probes appearing in the location of low salience bodies than probes in the location of high salience bodies (see Table 3 for mean RTs). These findings are consistent with prior evidence that emotional arousal can reduce top-down attention to salient stimuli in young adults (Sutherland et al., 2017). In contrast, for older adults, a trending non-significant one-sample *t*-test showed a negative attention bias score for body images ($M = -.016$, $SD = .05$) on non-arousing trials, $t(29) = -1.89$, $p = .06$, $d = -0.32$, implying quicker RTs to detect probes in the location of high versus low salience bodies on non-arousing trials. Older adults showed no attention bias for probes on arousing trials, $t = -.73$, $p = .47$. For scene images, young adults showed a negative bias score ($M = -.014$, $SD = .03$) on non-arousing trials, $t(29) = -2.74$, $p = .01$, but one-sample *t*-tests showed no other significant attention bias scores for scenes in young or older adults, $ts \leq -1.04$, $ps \geq .30$.

3.1.4 Incidental memory performance.[3]

Although our analyses focused primarily on hit rates and false alarm rates, all recognition performance indices, including gist hits and misses, are reported in Table 4 for completeness. According to the ANOVA on hit rates, there were main effects of arousal, salience, and stimulus type, which showed that hit rates were greater for images from arousing than non-arousing trials, $F(1, 58) = 4.52$, $p = .038$, $\eta_p^2 = .07$, for high salience than for low salience images, $F(1, 58) = 5.86$, $p = .019$, $\eta_p^2 = .09$, and for body than for scene images, $F(1, 58) = 8.49$, $p = .005$, $\eta_p^2 = .13$, respectively. There was also a four-way interaction of age group, arousal, salience, and stimulus type on hit rates, $F(1, 58) = 7.11$, $p = .010$, $\eta_p^2 = .11$, but there were no other significant effects or interactions, $Fs \leq 2.67$, $ps \geq .11$.

Since body and scene images belong to different stimuli categories with distinct cortical representations, we followed up the significant four-way interaction with separate age × arousal × salience ANOVAs for each stimulus type. For body images, there was an age × arousal × salience interaction, $F(1, 58) = 5.52$, $p = .02$, $\eta_p^2 = .09$ (Figure 4). Bonferroni-corrected pairwise comparisons showed that, for young adults, hit rates were greater for high salience body images than for low salience body images on arousing trials, $p = .04$, 95% *CI* [.003, .102], but not on non-arousing trials, $p = .52$, 95% *CI* [−.027, .053]. By

[2]As mentioned in the methods, one older adult's MRI data was not saved on the scanner due to a technical error. Although we could not include their imaging data, we included their behavioral data in our analyses.
[3]One older adult's recognition data was lost due to a technical error.

contrast, for older adults, hit rates were greater for high than for low salience body images on non-arousing trials, $p = .04$, 95% CI [.002, .083], but not on arousing trials, $p = .53$, 95% CI [−.065, .034]. For scene images, the age − arousal × salience ANOVA showed a trending non-significant main effect of salience, $F(1, 58) = 3.50$, $p = .06$, $\eta_p^2 = .06$, with greater hit rates for high than for low salience scene images. There were no other significant main effects or interactions for scenes, $Fs \leq 2.96$, $p \geq .09$.

Finally, false alarm rates were higher for body images ($M = .37$, $SD = .26$) than for scene images ($M = .27$, $SD = .27$), $F(1, 58) = 9.52$, $p = .003$, $\eta_p^2 = .141$. There was no main effect of age or an interaction of age and stimulus type, $Fs \leq 2.31$, $ps \geq .13$. Analysis of discrimination accuracy (hits minus false alarms) showed a main effect of stimulus, $F(1, 58) = 5.22$, $p = .03$, $\eta_p^2 = .08$. Discrimination accuracy was better for scene images ($M = -.10$, $SD = .17$) than for body images ($M = -.16$, $SD = .16$). There was no main effect of age group.

Together, these results suggest that arousal had a differential effect on memory selectivity as a function of age group as hypothesized. However, this age difference in memory selectivity on arousing trials was only observed for body images and not for scene images, which may be related to the biological relevance of body images (see Discussion section for more on this).

3.2 Brain Activity Results

3.2.1 Whole-brain activation during the incidental encoding task.—

Analysis of the BOLD signal at the whole-brain level revealed clusters showing a significant main effect of arousal on brain activity when participants were viewing the image pair. Arousing sounds increased activity in the frontal orbital cortex, supramarginal gyrus, superior and middle temporal gyrus, superior frontal gyrus, occipital fusiform gyrus, and the posterior cingulate gyrus. There was also an age-by-arousal interaction on incidental encoding-related activity such that young and older adults showed different patterns of brain activity on arousing relative to non-arousing trials. In young adults, arousing trials corresponded with increased activation of frontal and temporal regions including the superior frontal gyrus, temporal pole, and the middle temporal gyrus, whereas older adults showed greater activity in a more posterior region of the superior frontal gyrus as well as in the superior parietal lobule, middle frontal gyrus, and precuneus cortex (Figure 5 and Table 5).

There were main effects of salience for both body and scene images, confirming that the manipulation of perceptual contrast worked. When participants were viewing high relative to low salience body images, brain activity was greater in occipitotemporal regions consistent with the location of the EBA (Downing et al., 2001) including the right and left lateral occipital cortex, temporal occipital fusiform cortex, and inferior temporal gyrus. Similarly, when contrasting high salience scene images with low salience scene images, significant clusters emerged in the parahippocampal gyrus, the temporal occipital fusiform cortex, lingual gyrus, occipital pole, and precuneous cortex. These effects of salience did not differ as a function of age group or arousal level as no significant clusters were observed for these contrasts (Table 5).

Together, the whole-brain results showed that the arousing sounds were successful in activating brain regions involved in bottom-up attention, including areas in the ventral frontal cortex, more so than non-arousing sounds. The analysis also confirmed that the salience manipulation worked as there was greater activation for high versus low salience images in the expected category-selective regions (i.e., EBA and PPA) across age groups.

3.2.2 ROI analysis results.—Next, we analyzed how arousal modulated ROI activity including the LC, category-selective occipitotemporal regions, and the right TPJ. For the LC ROI, as hypothesized, there was a main effect of arousal, $F(1, 58) = 4.17$, $p = .046$, $\eta_p^2 = .07$, with higher LC activity on arousing than non-arousing trials. There was no significant effect of age group nor an interaction between age group and arousal, $Fs \leq .24$, $ps \geq .63$.

For the category-selective ROI analysis, there was a main effect of stimulus type, $F(1, 58)$ 36.09, $p < .001$, $\eta_p^2 = .38$, with greater activity in the EBA than PPA. There was also a significant interaction of age, arousal, salience, and stimulus type, $F(1, 58) = 7.81$, $p = .007$, $\eta_p^2 = .12$. To breakdown this interaction, separate age × arousal × salience ANOVAs were run for each stimulus type. For body images, a main effect of salience, $F(1, 58) = 33.62$, $p < .001$, $\eta_p^2 = .37$, indicated greater EBA activity for high relative to low salience body images. A significant three-way interaction of age, arousal, and salience, $F(1, 58) = 7.79$, $p = .007$, $\eta_p^2 = .12$, revealed that arousal's effect on EBA activity for high versus low salience body images differed between groups (Figure 6). As expected, Bonferroni-corrected pairwise comparisons revealed that EBA activity in young adults was greater for high than for low salience body images on arousing trials, $p < .001$, 95% CI [.041, .124], but not on non-arousing trials, $p = .36$, 95% CI [−.029, .077]. Older adults showed the opposite pattern: EBA activity was greater for high than for low salience body images on non-arousing trials, $p < .001$, 95% CI [.063, .169], but not on arousing trials, $p = .094$, 95% CI [−.006, .076]. These effects did not differ by hemisphere, $F = 1.09$, $p = .30$. high salience scene images evoked more PPA activity than low salience scene images, $F(1, 58) = 29.92$, $p < .001$, $\eta_p^2 = .34$. There was also a main effect of hemisphere, $F(1, 58) = 11.52$, $p = .001$, $\eta_p^2 = .16$, with greater activity in the right versus left PPA, but the critical age × arousal × salience interaction was not significant, $F = .01$, $p = .93$.

Finally, we examined age differences in the interaction of arousal and salience on activity in the right TPJ (rTPJ) in young and older adults. Given that we did not observe a three-way interaction in the behavioral and brain results for scene images, we focused this analysis on activity in the rTPJ when participants were viewing high versus low salience body images, since our analyses thus far have supported arousal-induced selectivity for body and not scene images. The analysis revealed a main effect of arousal, $F(1, 58) = 23.46$, $p < .001$, $\eta_p^2 = .29$, with significantly higher activity in the rTPJ on arousing trials versus non-arousing trials. There was also a significant three-way interaction between age, arousal, and salience, $F(1, 58) = 4.93$, $p = .03$, $\eta_p^2 = .08$. For young adults, pairwise comparisons showed increased activity in the rTPJ when viewing high salience body images on arousing versus non-arousing trials, $p = .021$, 95% CI [.047, .133]. For older adults, the effect was reversed: Activity in the rTPJ was enhanced for low salience body images on arousing versus non-arousing trials, $p = .007$, 95% CI [.016, .094]. In other words, arousal amplified activity in the rTPJ when young adults were viewing high versus low salience body images,

whereas no arousal-related modulation of rTPJ activity was observed for older adults. There were no other significant main effects or interactions, *ps* ≥ .17. These ROI findings align with behavioral results and our hypotheses, showing more selective activation in category-selective regions and in the rTPJ for high salience body images on arousing trials in young adults only.

3.2.3 LC contrast ratios.—The LC contrast ratios did not differ between young (M = .08, SD = .04) and older adults (M = .08, SD = .05), F = .01, p = .92, but ratios were higher in the left hemisphere (M = .10, SD = .05) than in the right hemisphere (M = .06, SD = .04), $F(1, 57) = 41.74$, $p < .001$, $\eta_p^2 = .42$. This replicates a previously reported lateralized effect (left > right) in LC ratios (Betts et al., 2017; Dahl et al., 2019).

3.2.4 Relationship between LC structure, LC function, pupil dilation, and behavior.—Pearson's correlation analysis showed that LC contrast ratios, averaged across hemispheres, were negatively associated with LC function on arousing trials in older adults, $r(29) = -0.415$, p = .025, but not in young adults, $r(30) = -0.066$, p = .728. According to Fisher's r-to-z transformation, the age difference between these correlation coefficients was not statistically significant, $Z = -1.37$, p = .085. The association between LC contrast ratios and LC function (both averaged across hemispheres) on neutral trials was not statistically significant in older adults, $r(29) = -0.317$, p =.094, nor in young adults, $r(30) = 0.116$, p = .542.

For both age groups, associations between LC contrast ratios, averaged across hemispheres, and pupil dilation were not statistically significant on arousing trials (older adults: $r(23) = -0.18$, p = .42; young adults: $r(29) = 0.06$, p = .76) or on neutral trials. LC function was positively associated with pupil dilation on arousing trials in young adults, $r(29) = 0.51$, p = .005, but not in older adults, $r(23) = 0.20$, p = .36. Fisher's r-to-z transformation indicated that these correlation coefficients were not statistically different across age groups, $Z = -1.24$, p = .11. There was no association between LC function and pupil dilation on neutral trials (older adults: $r(23) = 0.18$, p = .41; young adults: $r(29) = 0.16$, p = .41).

Finally, we tested the relationship between LC measures and memory selectivity. LC contrast ratios, averaged across hemispheres, were not associated with memory selectivity for body images on arousing trials (older adults: $r(28) = 0.08$, p = .67; young adults: $r(30) = 0.13$, p = .48), but they were positively associated with memory selectivity for body images on neutral trials in young, $r(30)$ = .41, p = .03, and not older adults, $r(28) = 0.19$, p = .33. Fisher's r-to-z transformation indicated that these correlation coefficients were not statistically different across age groups, $Z = 0.88$, p = .19. There were no statistically significant correlations between LC contrast and memory selectivity for scene images in either age group, *ps* > .38. There were also no statistically significant correlations between LC function and memory selectivity, *ps* > .21.

4. Discussion

How attention is modulated by the arousal system changes with age (Lee et al., 2018), which may arise from a combination of age-related neural changes. Older adults show functional

changes of critical attention networks in the brain (Campbell et al., 2012; Kennedy & Mather, 2019) that likely contribute to increases in distractibility and a reduced ability to focus on target information in aging (Hasher et al., 2007; Hasher & Zacks, 1988). Changes also occur in the LC-NA system during aging, including loss of LC integrity (Robertson, 2013) and increases in certain noradrenergic neurotransmitters that can influence attention and cognition (Mather, 2020). According to the GANE model, these age-related changes may make arousal less effective at amplifying selectivity in older compared to young adults (Mather et al., 2016). In the current study, we investigated age differences in the interaction of auditory-induced arousal with bottom-up (stimulus-driven) processing, top-down (goal-relevant) responses, and incidental memory. Our results revealed that arousal has a different effect on young and older adults' processing of high versus low salience stimuli.

4.1 Arousal-induced selectivity in attention and memory for young, not older adults

There was an arousal-induced selectivity effect for young but not older adults' category-selective brain activity and incidental memory performance. Young adults showed increased activity in the extrastriate body area when viewing high versus low salience body images on arousing trials. Older adults showed no such difference in their EBA activity as a function of salience on arousing trials. Instead, they showed enhanced EBA activity for high versus low salience body images after hearing a non-arousing sound. A similar arousal-related age difference was observed in the rTPJ, a node of the ventral attention network. On arousing relative to non-arousing trials, young adults' rTPJ activity was enhanced for high salience body images whereas older adults' rTPJ activity was enhanced for low salience body images. This is consistent with our hypothesis that arousal would enhance brain activity associated with bottom-up processing of high versus low salience images in young but not older adults. These findings also support the GANE model (Mather et al., 2016), illustrating how arousal can enhance neural processing of high over low priority mental representations in young adults.

While previous work testing GANE predictions (e.g., Lee et al., 2018) primarily focused on attention, the current project extends our understanding of arousal-induced selectivity to memory. Arousing trials amplified incidental memory for high versus low salience body images in young adults whereas older adults showed no such difference. Interestingly, older adults showed better memory for high than low salience body images after hearing a non-arousing sound, mirroring the EBA ROI results. This is an unexpected finding given previously reported age differences in the ability to ignore irrelevant (e.g., low salience) information (Hasher et al., 2007; Hasher & Zacks, 1988). One possibility is that older adults' baseline arousal level was higher than young adults. This could be due to changes in the LC-NA system with age (Mather, 2020) or elevated arousal in older adults from being inside the MRI scanner or in a novel lab environment (Sindi et al., 2013). This contrasts with young adults, many of which had participated in previous MRI studies. If older adults had higher baseline arousal than young adults, then we may be observing an arousal-related benefit on non-arousing trials in older adults. If so, further increases in arousal may have impaired their performance. Future research should measure age differences in baseline arousal at experiment onset to determine how these differences drive task performance.

Why did young adults show arousal-induced selectivity for body and not for scene images? One possibility is that bodies are more attention grabbing than scenes due to their biological relevance. This is consistent with the idea that perception is more sensitive to stimuli related to evolutionary fitness (Baluch & Itti, 2011) and biologically relevant stimuli (e.g., images relevant to survival or reproduction) have shown to modulate cognitive processes more automatically than socially relevant stimuli (e.g., images related to social adaptation; (Sakaki et al., 2012). Body images have also shown to hold attention longer, to be more rapidly processed (Ro et al., 2007) than other image types (e.g., clothes, appliances, food, plants; (Downing et al., 2004). Our results add to this by showing that arousal may enhance a bottom-up bias for biologically relevant body images. Although we did not observe arousal-induced selectivity for scenes, it is important to note other work has shown arousal-enhanced selective processing of scene images that were paired with object images (Lee et al., 2018). Our findings suggest that this effect may not be observed for certain stimulus categories when the competing stimulus is biologically relevant. Previous findings have shown a similar pattern, with arousal enhancing attention for living versus non-living stimuli (Sutherland et al., 2017).

It is also important to highlight that the age difference in the arousal-by-salience interaction in the EBA cannot be attributed to age-related changes in category-selective processing. Theories of age-related dedifferentiation propose that neural processes become less selective with age (Carp et al., 2011; Li et al., 2001). Yet we observed equivalent category-selective responses in young and older adults. In the whole-brain analysis, both age groups showed greater activation in category-selective occipitotemporal regions, including the EBA and PPA, when viewing high versus low salience body and scene images, respectively. Our results thus suggest that selective processing in these regions is intact in older adults and therefore cannot explain the age difference in arousal-induced selectivity (see also Lee et al., 2018).

Taken together, these ROI and incidental memory findings show that arousal did not enhance older adults' bottom-up processing of high relative to low salience images. Instead, arousal may enhance older adults' tendency to process all stimuli, regardless of salience. This could explain previous behavioral findings that older adults are more likely to process distracting information under arousing conditions than young adults (Durbin et al., 2018; Gallant et al., 2020). Arousal may therefore exacerbate age difficulties in inhibiting irrelevant or distracting stimuli (Hasher et al., 2007; Hasher & Zacks, 1988). Moreover, the current results highlight how young adults' arousal-induced selectivity extends to instances where priority is determined solely by perceptual salience and modulates rTPJ activity, a ventral frontoparietal region implicated in bottom-up orienting. This compliments and extends Lee et al.'s (2018) findings of age differences in how arousal influences neural selectivity in dorsal frontoparietal regions.

4.2 Arousal slowed young adults' detection of probes in the location of high salience images

We also analyzed arousal's impact on a top-down goal to detect probes appearing in the location of high versus low salience images. On arousing trials, young adults' attention

bias scores indicated that they were slower to detect probes appearing behind high than low salience body images than they were on non-arousing trials. This implies that arousal may have slowed as opposed to facilitated their ability to detect probes appearing behind high salience body images. This contrasts with older adults, who did not show a significant difference in their attention bias scores between arousing and non-arousing trials. This pattern of results in young adults is consistent with previous findings that high arousal can strengthen bottom-up representations (Lee et al., 2012, 2013; Sutherland & Mather, 2012; Sutherland et al., 2017) but can also interfere with top-down goals (Sutherland et al., 2017; Verbruggen & De Houwer, 2007). One possible reason for this could be that exposure to and processing of an arousing stimulus consumes executive control, leading to weakened top-down attention biases (Pessoa, 2009).

Another possibility is that young adults' slower RTs to detect high salience probes on arousing trials reflect an inhibition of return (IOR) effect. This inhibitory aftereffect occurs when attention is initially oriented to a high salience location but then is disengaged after a passage of time, resulting in delayed responding to information subsequently presented at the high salience location (Klein, 2000). In our task, it is possible that young adults' attention may have been initially captured by high over low salience images and then disengaged during the 500 ms ISI, leading to slower probe detection in the location of the high salience image. Future research with varied ISI lengths would be required to test this alternative explanation.

Taken together, arousal may have an inconsistent effect on bottom-up and top-down processing in young adults. Interestingly, we did not find significant effects of arousal on older adults' responses to probes appearing behind high versus low salience images. As not many studies have investigated the impact of aging on arousal induced-selectivity in top-down attention, further research is required to determine if there are indeed age differences.

4.3 No age differences in arousal-related responses or in LC measures

Relative to non-arousing sounds, both young and older adults in the current study showed higher subjective arousal ratings in response to arousing sounds. Measures of LC function were also similar across age groups as both pupil dilation and LC ROI activity were increased on arousing compared to non-arousing trials. Neuroimaging results further showed that, for both groups, arousing trials increased brain activity in regions consistent with the ventral attention network in the ventral frontal cortex and the rTPJ (Corbetta et al., 2008; Vossel et al., 2014) as well as the frontal orbital cortex, which is thought to play a role in driving phasic LC activation (Aston-Jones & Cohen, 2005). This implies that the age difference in arousal-induced selectivity in bottom-up processing and incidental memory cannot be attributed to age differences in the arousal response. It thus is unlikely that the *response* to arousal changes with age, but how effectively arousal coordinates brain activity involved in selective processing.

There were no age differences in LC contrast ratios. While age differences in LC contrast ratios have been observed (Clewett et al., 2016), others have found no difference in this measure of LC structure in healthy adults (Hämmerer et al., 2018). Studies using lifespan

samples have shown that LC MRI contrast has a quadratic relationship with age, peaking at 60 years, remaining stable until ~80 years, and gradually decreasing in the ninth decade (Liu et al., 2020; Shibata et al., 2006). Dividing our sample into distinct age groups may have therefore obscured age differences in LC contrast ratios that would have been captured by a lifespan sample.

Finally, a novel component of this study was the ability to test associations between LC MRI contrast and LC function. Given that LC MRI contrast is thought to reflect LC structural integrity (Liu et al., 2017), we expected this measure to correspond with LC ROI activity or pupil dilation, our independent measure of LC function (indeed, pupil dilation and LC ROI activity were positively correlated in young adults). However, we found no meaningful associations between LC structural MRI contrast and function. Our small sample size could explain why anticipated associations between LC measures were not present. Another contributing factor to these inconsistencies with prior work could be differences in imaging protocols used for structural LC assessment as well as the coordinates used for localizing LC function. Nevertheless, LC contrast ratios were associated with better memory selectivity on neutral trials in young adults, consistent with findings of a positive relationship between young adults' memory and LC MRI contrast (Clewett et al., 2018; Dahl et al., 2019). More research is needed to clarify the relationship between LC structure and function in young and older adults.

4.4 Limitations and Conclusions

There are some limitations to our study's design. We selected sound clips based on mean arousal and valence ratings provided by the IADS database but did not control for decibel (dB) level. One could argue that higher dB sounds exert a greater effect on the arousal response than lower dB sounds. However, a prior study using IADS sound clips found that the arousal level of sounds, and not their dB level, predicted recall performance of high and low salience stimuli in both young and older adults (Sutherland & Mather, 2015). Given the relevance of these findings to the current study, it seems unlikely that dB level impacted arousal-induced selectivity effects.

We also did not control for certain image-related factors, such as stimulus complexity, which can enhance recognition (Bender et al., 2017) in a manner similar to salience. There may have been trials where a high salience image was paired with a visually complex low salience image, which could have diminished a salience effect. However, such a pairing would have been unlikely to repeat for another participant given that image pairing was randomized. It is therefore more likely that such differences in image complexity added noise to the data that reduced power rather than confounding our results.

Concerning the salience manipulation of image contrast, we did not control for individual differences in visual contrast sensitivity, or the ability to distinguish between an object and its background. One might argue that, if an individual had reduced visual contrast sensitivity, they might have difficulty perceiving the low salience images with degraded contrast. As all participants reported having normal or corrected-to-normal vision, we do not believe that this confounded our results; however, future studies might consider including a measure

of visual contrast sensitivity to determine if such individual differences affect attention selectivity based on image salience.

Finally, in terms of analyses, we did not look at incidental encoding-related activation as a function of subsequent memory performance. Our findings thus cannot speak to how arousal modulates brain activity patterns that predict remembering and forgetting of high versus low salience stimuli. We took this approach to analyze activation irrespective of memory outcome to increase power as memory performance was poor. This is evident given that hit rates for all conditions were below chance levels for both age groups and discrimination accuracy scores (hits minus false alarms) were below zero. As such, memory outcomes from this task should be interpreted with caution. This outcome was somewhat expected given the memory task was incidental and participants were not aware it would occur. The low memory performance could also be explained by the complexity of the incidental encoding task, which involved multiple components (i.e., hearing an arousing sound, perceiving high and low salience images, and detecting a probe). Nevertheless, the memory outcomes for body images align closely with previous studies showing arousal-induced selectivity in memory (Clewett et al., 2018; Durbin et al., 2018). To draw conclusions about the link between perception and memory in the brain, future research should use a task with sufficient power to conduct a subsequent memory analysis of fMRI data.

In conclusion, our findings indicate a dissociation in the way that arousal modulates selectivity in young and older adults' behavior, category-selective processing, and ventral attention network activity. During increased emotional arousal, young adults are better able to process high salience information, whereas older adults' attention becomes less selective. Although older adults tend to show poorer selective attention and increased distractibility than young adults (Hasher & Zacks, 1988), our results suggest that arousal may further exacerbate this vulnerability. In turn, older adults may be less able to focus during arousing situations, whether evoked by stimuli associated with an aversive event (Lee et al., 2018), a threat of punishment (Durbin et al., 2018), or from hearing an emotionally arousing sound. This could have detrimental consequences for older adults' performance in high-stake moments.

Supplementary Material

Refer to Web version on PubMed Central for supplementary material.

Acknowledgements

This research was supported by a BrightFocus Postdoctoral Fellowship (A2018449F) awarded to SG with partial support from Alzheimer's Los Angeles. BK was supported by a National Institutes of Health grant (F32AG057162). SB was supported by National Science Foundation grant DGE-1842487 and National Institutes of Health grant T32AG000037. MM was supported by a National Institutes of Health grant (R01AG025340). We thank Taylor Shigezawa and Ilana Cohen for assistance with neuroimaging preprocessing and manual LC delineation as well as Katherin Martin for her help with MRI acquisition.

References

Aston-Jones G, & Cohen JD (2005). Adaptive gain and the role of the locus coeruleus-norepinephrine system in optimal performance. The Journal of Comparative Neurology, 493(1), 99–110. 10.1002/cne.20723 [PubMed: 16254995]

Avants BB, Tustison N, & Song G (2009). Advanced Normalization Tools (ANTS). The Insight Journal, 2(365), 1–35.

Baluch F, & Itti L (2011). Mechanisms of top-down attention. In Trends in Neurosciences (Vol. 34, Issue 4, pp. 210–224). 10.1016/j.tins.2011.02.003 [PubMed: 21439656]

Bates D, Mächler M, Bolker BM, & Walker SC (2015). Fitting linear mixed-effects models using lme4. Journal of Statistical Software, 67(1). 10.18637/jss.v067.i01

Beckmann CF, Jenkinson M, & Smith SM (2003). General multilevel linear modeling for group analysis in FMRI. NeuroImage, 20, 1052–1063. 10.1016/S1053-8119(03)00435-X [PubMed: 14568475]

Beckmann CF, & Smith SM (2004). Probabilistic independent component analysis for functional magnetic resonance imaging. IEEE Transactions on Medical Imaging, 23(2), 137–152. 10.1109/tmi.2003.822821 [PubMed: 14964560]

Bender AR, Naveh-Benjamin M, Amann K, & Raz N (2017). The role of stimulus complexity and salience in memory for face-name associations in healthy adults: Friend or foe? Psychology and Aging, 32(5), 489–505. 10.1037/pag0000185 [PubMed: 28816475]

Betts MJ, Cardenas-blanco A, Kanowski M, Jessen F, & Düzel E (2017). In vivo MRI assessment of the human locus coeruleus along its rostrocaudal extent in young and older adults. NeuroImage, 163, 150–159. 10.1016/j.neuroimage.2017.09.042 [PubMed: 28943414]

Bowling JT, Friston KJ, & Hopfinger JB (2020). Top-down versus bottom-up attention differentially modulate frontal–parietal connectivity. Human Brain Mapping, 41(4), 928–942. 10.1002/hbm.24850 [PubMed: 31692192]

Bradley MM, & Lang PJ (2007). The International Affective Digitized Sounds (2nd Edition; IADS-2): Affective ratings of sounds and instruction manual (Technical report B-3.). University of Florida, Gainesville, Fl.

Campbell KL, Grady CL, Ng C, & Hasher L (2012). Age differences in the frontoparietal cognitive control network: Implications for distractibility. Neuropsychologia, 50(9), 2212–2223. 10.1016/j.neuropsychologia.2012.05.025 [PubMed: 22659108]

Carp J, Park J, Polk TA, & Park DC (2011). Age differences in neural distinctiveness revealed by multi-voxel pattern analysis. NeuroImage, 56(2), 736–743. 10.1016/j.neuroimage.2010.04.267 [PubMed: 20451629]

Clewett DV, Huang R, Velasco R, Lee TH, & Mather M (2018). Locus coeruleus activity strengthens prioritized memories under arousal. Journal of Neuroscience, 38(6), 1558–1574. 10.1523/JNEUROSCI.2097-17.2017 [PubMed: 29301874]

Clewett DV, Lee TH, Greening S, Ponzio A, Margalit E, & Mather M (2016). Neuromelanin marks the spot: identifying a locus coeruleus biomarker of cognitive reserve in healthy aging. Neurobiology of Aging, 37, 117–126. 10.1016/j.neurobiolaging.2015.09.019 [PubMed: 26521135]

Corbetta M, Patel G, & Shulman GL (2008). The reorienting system of the human brain: From environment to theory of mind. Neuron, 58(3), 306–324. 10.1016/j.neuron.2008.04.017 [PubMed: 18466742]

Corbetta M, & Shulman GL (2002). Control of goal-directed and stimulus-driven attention in the brain. Nature Reviews. Neuroscience, 3(3), 201–215. 10.1038/nrn755 [PubMed: 11994752]

Dahl MJ, Mather M, Düzel S, Bodammer NC, Lindenberger U, Kühn S, & Werkle-Bergner M (2019). Rostral locus coeruleus integrity is associated with better memory performance in older adults. Nature Human Behaviour, 3(11), 1203–1214. 10.1038/s41562-019-0715-2

Dahl MJ, Mather M, Werkle- Bergner M, Kennedy BL, Qiao Y, Shi Y, & Ringman JM (2020). Lower MRI- indexed locus coeruleus integrity in autosomal- dominant Alzheimer's disease. In Alzheimer's & Dementia (Vol. 16, Issue S5). 10.1002/alz.047676

Damoiseaux JS, Beckmann CF, Arigita EJS, Barkhof F, Scheltens P, Stam CJ, Smith SM, & Rombouts SARB (2008). Reduced resting-state brain activity in the “default network” in normal aging. Cerebral Cortex , 18(8), 1856–1864. 10.1093/cercor/bhm207 [PubMed: 18063564]

Downing PE, Bray D, Rogers J, & Childs C (2004). Bodies capture attention when nothing is expected. Cognition, 93(1), 27–38. 10.1016/j.cognition.2003.10.010

Downing PE, Chan AWY, Peelen MV, Dodds CM, & Kanwisher N (2006). Domain specificity in visual cortex. Cerebral Cortex , 16(10), 1453–1461. 10.1093/cercor/bhj086 [PubMed: 16339084]

Downing PE, Jiang Y, Shuman M, & Kanwisher N (2001). A cortical area selective for visual processing of the human body. Science, 293(5539), 2470–2473. 10.1126/science.1063414\r293/5539/2470 [pii] [PubMed: 11577239]

Durbin KA, Clewett D, Huang R, & Mather M (2018). Age differences in selective memory of goal-relevant stimuli under threat. Emotion , 18(6), 906–911. 10.1037/emo0000398 [PubMed: 29389199]

Epstein R, & Kanwisher NG (1998). A cortical representation of the local visual environment. Nature, 392(6676), 598–601. 10.1038/33402 [PubMed: 9560155]

Fox MD, Corbetta M, Snyder AZ, Vincent JL, & Raichle ME (2006). Spontaneous neuronal activity distinguishes human dorsal and ventral attention systems. Proceedings of the National Academy of Sciences of the United States of America, 103(26), 10046–10051. 10.1073/pnas.0604187103 [PubMed: 16788060]

Gallant SN, Durbin KA, & Mather M (2020). Age differences in vulnerability to distraction under arousal. Psychology and Aging, 35(5), 780–791. 10.1037/pag0000426 [PubMed: 32744858]

Griffanti L, Douaud G, Bijsterbosch J, Evangelisti S, Alfaro-Almagro F, Glasser MF, Duff EP, Fitzgibbon S, Westphal R, Carone D, Beckmann CF, & Smith SM (2017). Hand classification of fMRI ICA noise components. NeuroImage, 154, 188–205. 10.1016/j.neuroimage.2016.12.036 [PubMed: 27989777]

Hämmerer D, Callaghan MF, Hopkins A, Kosciessa J, Betts M, Cardenas-Blanco A, Kanowski M, Weiskopf N, Dayan P, Dolan RJ, Düzel E, Kanowski M, Kosciessa J, Betts M, Callaghan MF, Düzel E, Hopkins A, Weiskopf N, & Hämmerer D (2018). Locus coeruleus integrity in old age is selectively related to memories linked with salient negative events. Proceedings of the National Academy of Sciences of the United States of America, 115(9), 2228–2233. 10.1073/pnas.1712268115 [PubMed: 29440429]

Hasher L, Lustig C, & Zacks RT (2007). Inhibitory mechanisms and the control of attention. In Conway ARA, Jarrold C, Kane MJ, Miyake A, & Towse JN (Eds.), Variation in working memory (pp. 227–249). Oxford University Press.

Hasher L, & Zacks RT (1988). Working memory, comprehension, and aging: A review and a new view. Psychology of Learning and Motivation, 22, 193–225. 10.1016/S0079-7421(08)60041-9

Itti L, & Koch C (2000). A saliency-based search mechanism for overt and covert shifts of visual attention. Vision Research, 40(10–12), 1489–1506. 10.1016/s0042-6989(99)00163-7 [PubMed: 10788654]

Jacobs HIL, Priovoulos N, Poser BA, Pagen LHG, Ivanov D, Verhey FRJ, & Uludağ K (2020). Dynamic behavior of the locus coeruleus during arousal-related memory processing in a multi-modal 7T fMRI paradigm. ELife, 9, 1–30. 10.7554/eLife.52059

Jenkinson M, Bannister P, Brady M, & Smith S (2002). Improved optimization for the robust and accurate linear registration and motion correction of brain images. NeuroImage, 17, 825–841. 10.1006/nimg.2002.1132 [PubMed: 12377157]

Johnson MR, Mitchell KJ, Raye CL, D’Esposito M, & Johnson MK (2007). A brief thought can modulate activity in extrastriate visual areas: Top-down effects of refreshing just-seen visual stimuli. NeuroImage, 37(1), 290–299. 10.1016/j.neuroimage.2007.05.017 [PubMed: 17574442]

Kahnt T, & Tobler PN (2013). Salience signals in the right temporoparietal junction facilitate value-based decisions. Journal of Neuroscience, 33(3), 863–869. 10.1523/JNEUROSCI.3531-12.2013 [PubMed: 23325225]

Kaiser D, Strnad L, Seidl KN, Kastner S, & Peelen MV (2014). Whole person-evoked fMRI activity patterns in human fusiform gyrus are accurately modeled by a linear combination of face- and body-evoked activity patterns. Journal of Neurophysiol, 111, 82–90. 10.1152/jn.00371.2013

Kennedy BL, & Mather M (2019). Neural mechanisms underlying age-related changes in attentional selectivity. In Samanez-Larkin GR (Ed.), The aging brain: Functional adaptation across adulthood (pp. 45–72). American Psychological Association. 10.1037/0000143-003

Keren NI, Lozar CT, Harris KC, Morgan PS, & Eckert MA (2009). In vivo mapping of the human locus coeruleus. NeuroImage, 47(4), 1261–1267. 10.1016/j.neuroimage.2009.06.012 [PubMed: 19524044]

Klein RM (2000). Inhibition of return. Trends in Cognitive Sciences, 4(4), 138–147. 10.1016/S1364-6613(00)01452-2 [PubMed: 10740278]

Kuznetsova A, Brockhoff PB, & Christensen RHB (2017). lmerTest package: Tests in linear mixed effects models. Journal of Statistical Software, 82(13). 10.18637/jss.v082.i13

Lee TH, Greening SG, Ueno T, Clewett D, Ponzio A, Sakaki M, & Mather M (2018). Arousal increases neural gain via the locus coeruleus-noradrenaline system in younger adults but not in older adults. Nature Human Behaviour, 2(5), 356–366. 10.1038/s41562-018-0344-1

Lee TH, Itti L, & Mather M (2012). Evidence for arousal-biased competition in perceptual learning. Frontiers in Psychology, 3(Article 241), 1–9. 10.3389/fpsyg.2012.00241 [PubMed: 22279440]

Lee TH, Sakaki M, Cheng R, Velasco R, & Mather M (2013). Emotional arousal amplifies the effects of biased competition in the brain. Social Cognitive and Affective Neuroscience, 9(12), 2067–2077. 10.1093/scan/nsu015

Li SC, Lindenberger U, & Sikström S (2001). Aging cognition: from neuromodulation to representation. Trends in Cognitive Sciences, 5(11), 479–486. 10.1016/s1364-6613(00)01769-1 [PubMed: 11684480]

Liu KY, Kievit RA, Tsvetanov KA, Betts MJ, Düzel E, Rowe JB, Tyler LK, Brayne C, Bullmore ET, Calder AC, Cusack R, Dalgleish T, Duncan J, Henson RN, Matthews FE, Marslen-Wilson WD, Rowe JB, Shafto MA, Campbell K, … Hämmerer D (2020). Noradrenergic-dependent functions are associated with age-related locus coeruleus signal intensity differences. Nature Communications, 11(1), 1–9. 10.1038/s41467-020-15410-w

Liu KY, Marijatta F, Hämmerer D, Acosta-Cabronero J, Düzel E, & Howard RJ (2017). Magnetic resonance imaging of the human locus coeruleus: A systematic review. Neuroscience and Biobehavioral Reviews, 83(September), 325–355. 10.1016/j.neubiorev.2017.10.023 [PubMed: 29107830]

Lovibond PF, & Lovibond SH (1995). The structure of negative emotional states: Comparison of the Depression Anxiety Stress Scales (DASS) with the Beck Depression and Anxiety Inventories. Behaviour Research and Therapy, 33(3), 335–343. 10.1016/0005-7967(94)00075-U [PubMed: 7726811]

Mars RB, Sallet J, Schüffelgen U, Jbabdi S, Toni I, & Rushworth MFS (2012). Connectivity-based subdivisions of the human right “temporoparietal junction area”: Evidence for different areas participating in different cortical networks. Cerebral Cortex, 22(8), 1894–1903. 10.1093/cercor/bhr268 [PubMed: 21955921]

Mather M (2020). The locus coeruleus-norepinephrine system role in cognition and how it changes with aging. In Poeppel D, Mangun G, & Gazzaniga M (Eds.), The Cognitive Neurosciences (6th ed., pp. 91–104). The MIT Press. https://www.ncbi.nlm.nih.gov/pubmed/25246403

Mather M, & Carstensen LL (2003). Aging and attentional biases for emotional faces. Psychological Science, 14(5), 409–415. 10.1111/1467-9280.01455 [PubMed: 12930469]

Mather M, Clewett D, Sakaki M, & Harley CW (2016). Norepinephrine ignites local hotspots of neuronal excitation: How arousal amplifies selectivity in perception and memory. The Behavioral and Brain Sciences, 39(200). 10.1017/S0140525X15000667

Mather M, & Sutherland MR (2011). Arousal-biased competition in perception and memory. Perspectives on Psychological Science: A Journal of the Association for Psychological Science, 6(2), 114–133. 10.1177/1745691611400234 [PubMed: 21660127]

Mathôt S, van der Linden L, Grainger J, & Vitu F (2013). The pupillary light response reveals the focus of covert visual attention. PloS One, 8(10). 10.1371/journal.pone.0078168

Meteyard L, & Davies RAI (2020). Best practice guidance for linear mixed-effects models in psychological science. Journal of Memory and Language, 112(March 2019), 104092. 10.1016/j.jml.2020.104092

Murphy PR, O'Connell RG, O'Sullivan M, Robertson IH, & Balsters JH (2014). Pupil diameter covaries with BOLD activity in human locus coeruleus. Human Brain Mapping, 35(8), 4140–4154. 10.1002/hbm.22466 [PubMed: 24510607]

Nasreddine ZS, Phillips NA, Bédirian V, Charbonneau S, Whitehead V, Collin I, Cummings JL, & Chertkow H (2005). The Montreal Cognitive Assessment, MoCA: A brief screening tool for mild cognitive impairment. Journal of the American Geriatrics Society, 53(4), 695–699. 10.1111/j.1532-5415.2005.53221.x [PubMed: 15817019]

Nieuwenhuis S, Aston-Jones G, & Cohen JD (2005). Decision making, the P3, and the locus coeruleus-norepinephrine system. Psychological Bulletin, 131(4), 510–532. 10.1037/0033-2909.131.4.510 [PubMed: 16060800]

Orlov T, Makin TR, & Zohary E (2010). Topographic Representation of the Human Body in the Occipitotemporal Cortex. Neuron, 68(3), 586–600. 10.1016/j.neuron.2010.09.032 [PubMed: 21040856]

Pessoa L (2009). How do emotion and motivation direct executive control? Trends in Cognitive Sciences, 13(4), 160–166. 10.1016/j.tics.2009.01.006 [PubMed: 19285913]

Ptak R (2012). The frontoparietal attention network of the human brain: Action, saliency, and a priority map of the environment. The Neuroscientist: A Review Journal Bringing Neurobiology, Neurology and Psychiatry, 18(5), 502–515. 10.1177/1073858411409051 [PubMed: 21636849]

Ro T, Friggel A, & Lavie N (2007). Attentional biases for faces and body parts. Visual Cognition, 15(3), 322–348. 10.1080/13506280600590434

Robertson IH (2013). A noradrenergic theory of cognitive reserve: Implications for Alzheimer's disease. Neurobiology of Aging, 34(1), 298–308. 10.1016/j.neurobiolaging.2012.05.019 [PubMed: 22743090]

Sakaki M, Niki K, & Mather M (2012). Beyond arousal and valence: the importance of the biological versus social relevance of emotional stimuli. Cognitive, Affective & Behavioral Neuroscience, 12(1), 115–139. 10.3758/s13415-011-0062-x

Samuels E, & Szabadi E (2008). Functional neuroanatomy of the noradrenergic locus coeruleus: Its roles in the regulation of arousal and autonomic function part I: Principles of functional organisation. Current Neuropharmacology, 6(3), 235–253. 10.2174/157015908785777229 [PubMed: 19506723]

Sara SJ (2009). The locus coeruleus and noradrenergic modulation of cognition. Nature Reviews. Neuroscience, 10(3), 211–223. 10.1038/nrn2573 [PubMed: 19190638]

Sara SJ, & Bouret S (2012). Orienting and reorienting: The locus coeruleus mediates cognition through arousal. Neuron, 76(1), 130–141. 10.1016/j.neuron.2012.09.011 [PubMed: 23040811]

Sasaki M, Shibata E, Tohyama K, Takahashi J, Otsuka K, Tsuchiya K, Takahashi S, Ehara S, Terayama Y, & Sakai A (2006). Neuromelanin magnetic resonance imaging of locus ceruleus and substantia nigra in Parkinson's disease. Neuroreport, 17(11), 1215–1218. 10.1097/01.wnr.0000227984.84927.a7 [PubMed: 16837857]

Shibata E, Sasaki M, Tohyama K, Kanbara Y, Otsuka K, Ehara S, & Sakai A (2006). Age-related changes in locus ceruleus on neuromelanin magnetic resonance imaging at 3 Tesla. Magnetic Resonance in Medical Sciences: MRMS: An Official Journal of Japan Society of Magnetic Resonance in Medicine, 5(4), 197–200. 10.2463/mrms.5.197 [PubMed: 17332710]

Shipley WC (1940). A self-administering scale for measuring intellectual impairment and deterioration. The Journal of Psychology, 9(2), 371–377. 10.1080/00223980.1940.9917704

Shomstein S (2012). Cognitive functions of the posterior parietal cortex: Top-down and bottom-up attentional control. Frontiers in Integrative Neuroscience, 6(Article 38), 1–7. 10.3389/fnint.2012.00038 [PubMed: 22319479]

Sindi S, Fiocco AJ, Juster R-P, Pruessner J, & Lupien SJ (2013). When we test, do we stress? Impact of the testing environment on cortisol secretion and memory performance in older adults. Psychoneuroendocrinology, 38(8), 1388–1396. 10.1016/j.psyneuen.2012.12.004 [PubMed: 23352228]

Snodgrass JG, & Corwin J (1988). Pragmatics of Measuring Recognition Memory: Applications to Dementia and Amnesia. Journal of Experimental Psychology. General, 117(1), 34–50. 10.1037/0096-3445.117.1.34 [PubMed: 2966230]

Strange BA, & Dolan RJ (2007). B-adrenergic modulation of oddball responses in humans. Behavioral and Brain Functions: BBF, 3(29), 1–5. 10.1186/1744-9081-3-29 [PubMed: 17214890]

Sutherland MR, & Mather M (2012). Negative arousal amplifies the effects of saliency in short-term memory. Emotion , 12(6), 1367–1372. 10.1037/a0027860 [PubMed: 22642352]

Sutherland MR, & Mather M (2015). Negative arousal increases the effects of stimulus salience in older adults. Experimental Aging Research, 41(3), 259–271. 10.1080/0361073X.2015.1021644 [PubMed: 25978446]

Sutherland MR, Mcquiggan DA, Ryan JD, Mather M, Sutherland MR, Mcquiggan DA, Ryan JD, & Mather M (2017). Perceptual salience does not influence emotional arousal's impairing effects on top-down. Emotion , 16(4), 700–706. 10.1037/emo0000245

Taylor JC, Wiggett AJ, & Downing PE (2007). Functional MRI analysis of body and body part representations in the extrastriate and fusiform body areas. Journal of Neurophysiology, 98(3), 1626–1633. 10.1152/jn.00012.2007 [PubMed: 17596425]

Vazey EM, Moorman DE, & Aston-Jones G (2018). Phasic locus coeruleus activity regulates cortical encoding of salience information. Proceedings of the National Academy of Sciences of the United States of America, 115(40), E9439–E9448. 10.1073/pnas.1803716115 [PubMed: 30232259]

Verbruggen F, & De Houwer J (2007). Do emotional stimuli interfere with response inhibition? Evidence from the stop signal paradigm. Cognition and Emotion, 21(2), 391–403. 10.1080/02699930600625081

Vossel S, Geng JJ, & Fink GR (2014). Dorsal and ventral attention systems: Distinct neural circuits but collaborative roles. The Neuroscientist: A Review Journal Bringing Neurobiology, Neurology and Psychiatry, 20(2), 150–159. 10.1177/1073858413494269 [PubMed: 23835449]

Willenbockel V, Sadr J, Fiset D, Horne GO, Gosselin F, & Tanaka JW (2010). Controlling low-level image properties: The SHINE toolbox. Behavior Research Methods, 42(3), 671–684. 10.3758/BRM.42.3.671 [PubMed: 20805589]

Wojciulik E, Kanwisher N, & Driver J (1998). Covert visual attention modulates face-specific activity in the human fusiform gyrus: fMRI study. Journal of Neurophysiology, 79(3), 1574–1578. 10.1152/jn.1998.79.3.1574 [PubMed: 9497433]

Xiao J, Hays J, Ehinger KA, Oliva A, & Torralba A (2010). SUN database: Large-scale scene recognition from abbey to zoo. Proceedings of the IEEE Computer Society Conference on Computer Vision and Pattern Recognition, 3485–3492. 10.1109/CVPR.2010.5539970

Ye R, Rua C, Callaghan CO, Jones PS, Hezemans FH, Kaalund SS, Tsvetanov KA, Rodgers CT, Williams G, Passamonti L, & Rowe JB (2021). An in vivo probabilistic atlas of the human locus coeruleus at ultra-high field. NeuroImage, 225, 117487. 10.1016/j.neuroimage.2020.117487 [PubMed: 33164875]

Yi D-J, & Chun MM (2005). Attentional modulation of learning-related repetition attenuation effects in human parahippocampal cortex. The Journal of Neuroscience: The Official Journal of the Society for Neuroscience, 25(14), 3593–3600. 10.1523/JNEUROSCI.4677-04.2005 [PubMed: 15814790]

Highlights

- In young adults, selective attention to high salience information is amplified by arousal
- Age-related changes in arousal and attention may hinder this selectivity effect
- We tested age differences in arousal's effect on cognitive and neural selectivity
- Older adults showed less selectivity under arousal than young adults
- Increases in arousal may exacerbate age-related vulnerability to distraction

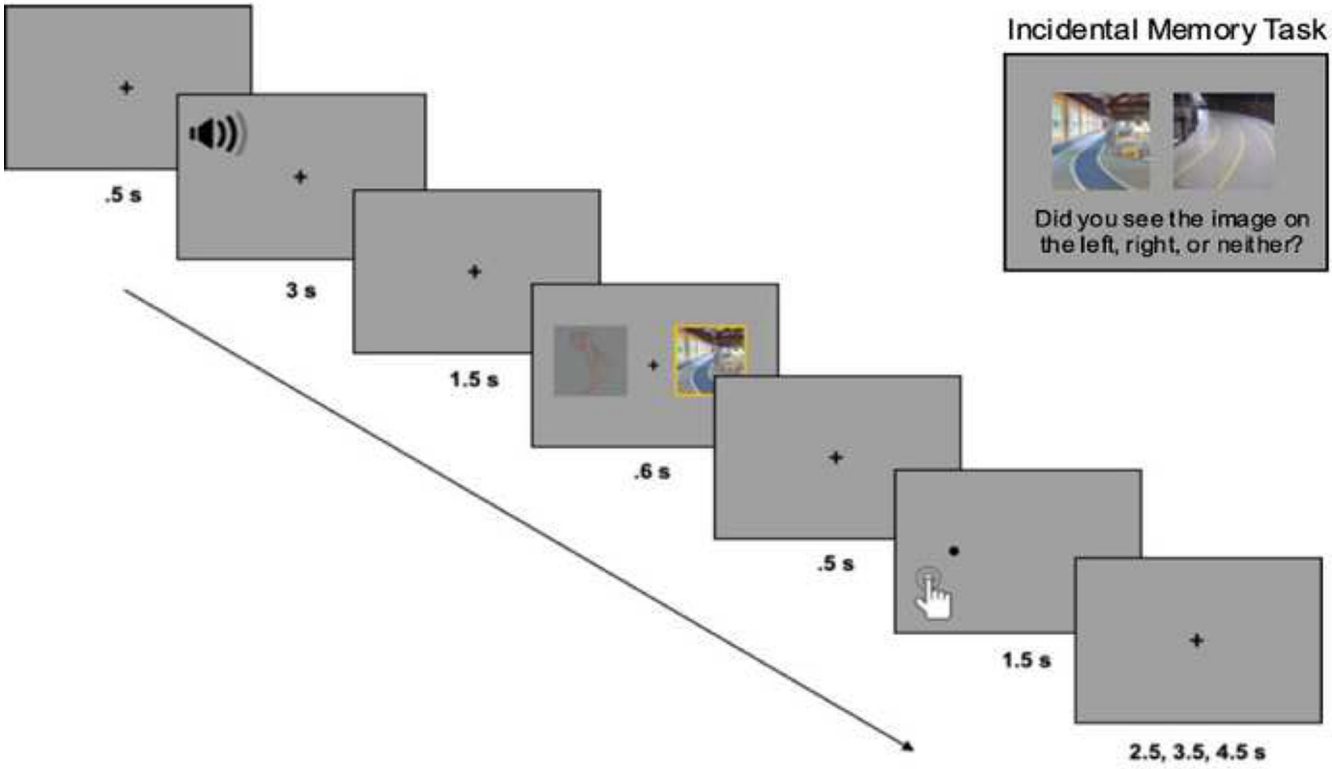

Figure 1.
Sample trials from the incidental encoding task and recognition task.

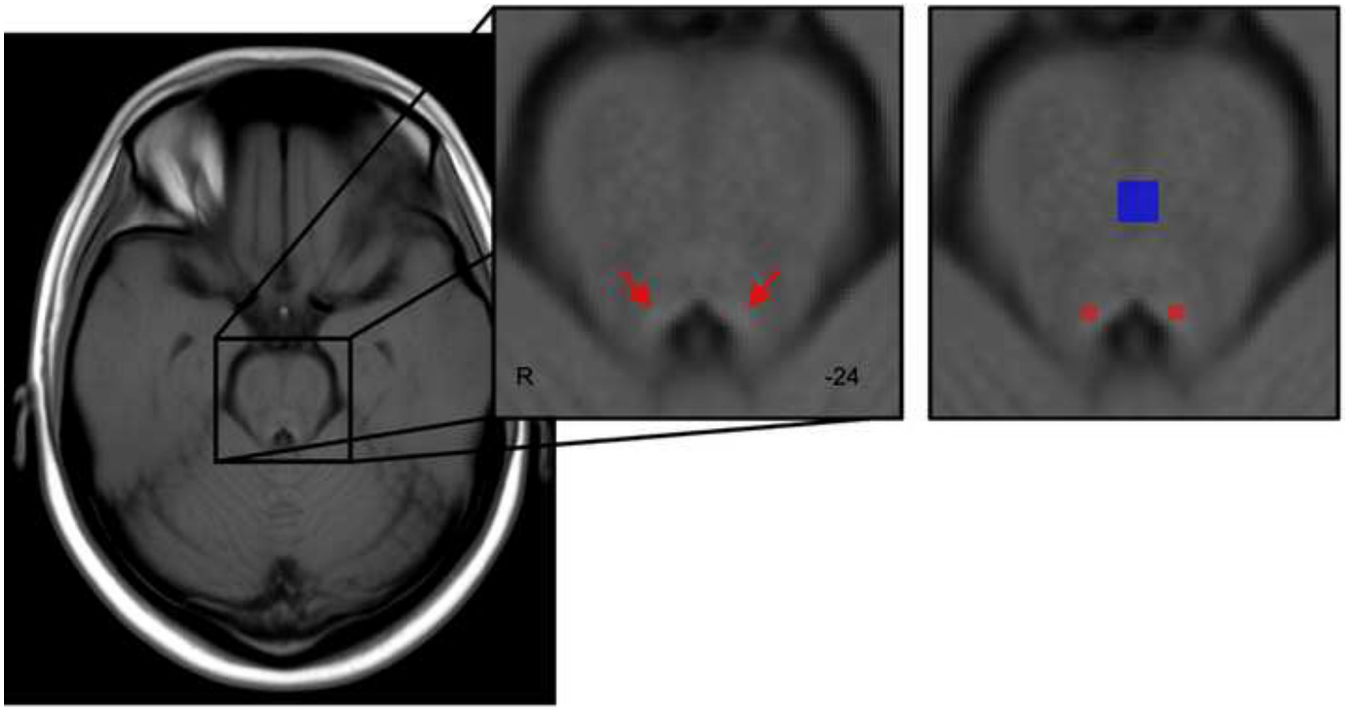

Figure 2.

Template of all participants' TSE scans, warped to MNI152 0.5mm linear space in the axial plane. Red arrows indicate hyperintensities bordering the fourth ventricle. For calculation of LC contrast ratios, a previously published LC map (Keren et al., 2009) was applied as a mask on individual TSE scans (shown in red) to identify probable voxels corresponding to the LC. In addition, a reference region covering the central pons (Dahl et al., 2020) was applied as a mask on individual TSE scans (shown in blue). Peak intensities within the masked LC and reference regions were extracted for each participant to calculate contrast ratios.

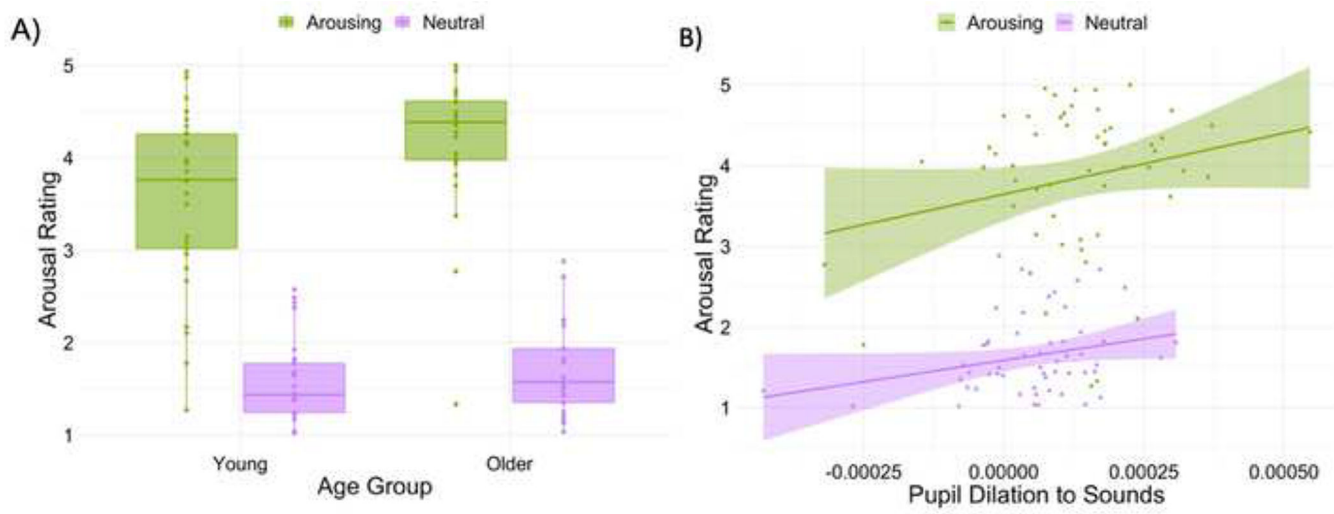

Figure 3.

Results from linear mixed-effects model of subjective and objective arousal responses to sounds. A) Boxplots display the age × arousal interaction. Crossbars represent medians and the upper and lower hinges correspond to first and third quartiles, respectively. B) A significant arousal × pupil interaction showed that pupil dilation evoked by arousing sounds were more associated with subjective ratings than pupil dilation evoked by non-arousing sounds. Lines and shaded areas represent regression fits and standard error, respectively. For both plots, each dot represents a participant.

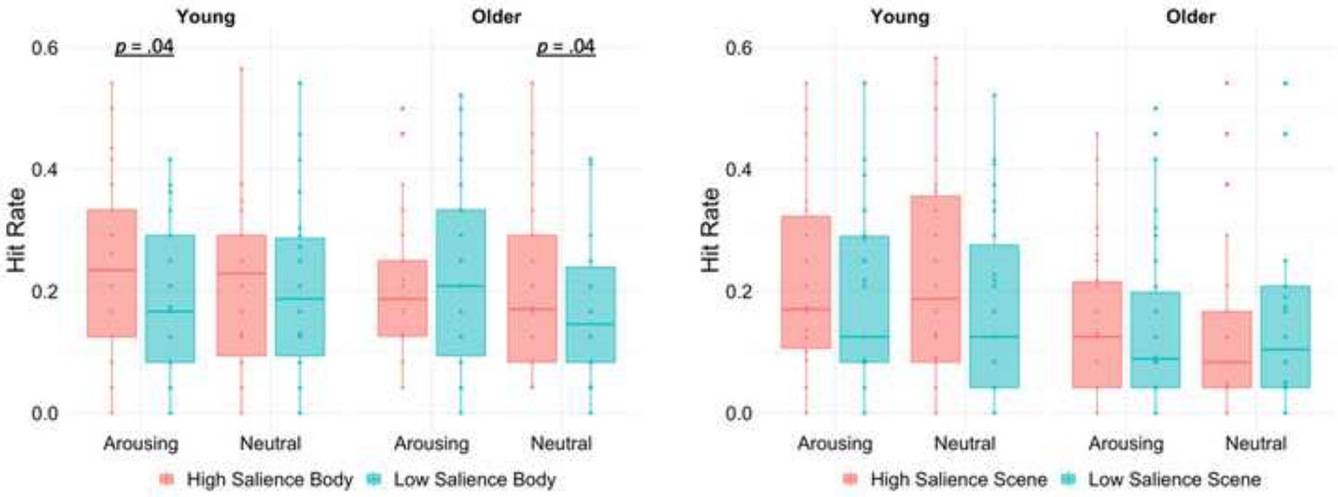

Figure 4.

Box plots display recognition hit rates for body and scene images as a function of age group, arousal, and salience. Crossbars represent medians and the upper and lower hinges correspond to first and third quartiles, respectively. Each dot represents a single participant.

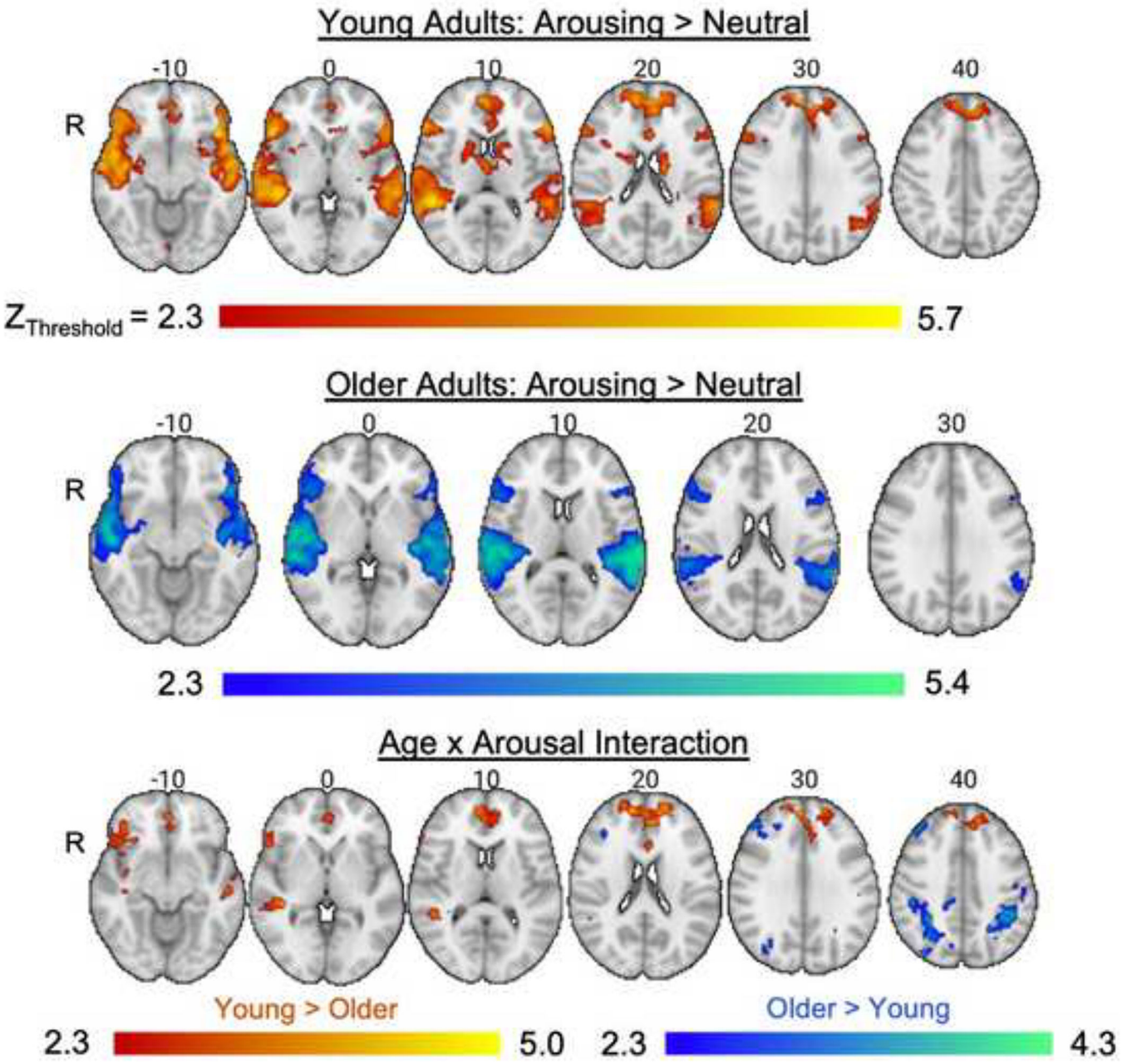

Figure 5.

Whole-brain analysis results illustrating the effects of arousing sounds on brain activity when viewing images during the incidental encoding task. The age × arousal interaction displays brain regions where age groups differed in the contrast of arousing versus non-arousing trials.

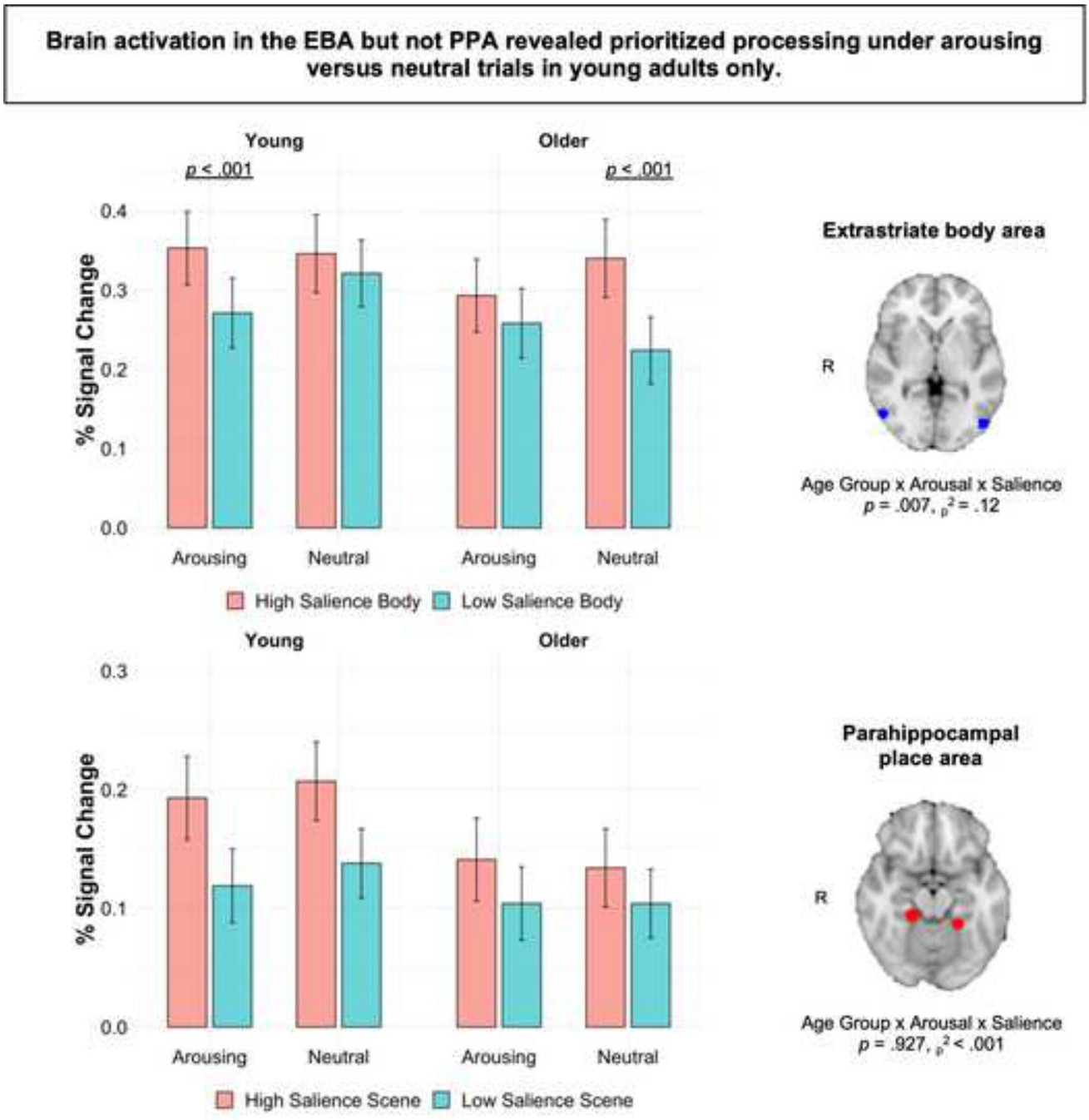

Figure 6.

Mean percent signal change ± SEM in the EBA and PPA while viewing image pairs during the incidental encoding task. The significant age × arousal × salience interaction for the EBA shows that arousing sounds enhanced prioritized processing in young adults, whereas older adults showed prioritized processing on trials with non-arousing sounds. There was no evidence for arousal-modulated processing in the PPA.

Table 1

Sample Characteristics

Characteristic	Young Adults M (SD)	Older Adults M (SD)	Group Difference
Age	23.43 (2.84)	70.63 (6.16)	t(58) = −38.14, p < .001
Sex ratio	18F:12M	15F:15M	χ (1) = .27, p = .60
Years of education	16.77 (2.34)	17.90 (3.10)	t(58) = −1.59, p = .12
Vocabulary level [a]	31.23 (3.41)	35.50 (3.49)	t(58) = −4.78, p < .001
Depression [b]	6.07 (7.13)	3.80 (5.64)	t(58) = 1.36, p = .18
Anxiety [b]	5.27 (5.19)	2.80 (3.31)	t(58) = 2.19, p = .03
Stress [b]	9.53 (7.18)	6.93 (5.22)	t(58) = 1.61, p = .11
MoCA [c]	28.50 (1.22)	26.79 (2.23)	t(56) = 3.66, p = .001

Note.

[a] Assessed with Shipley Vocabulary test (total possible = 40)

[b] Assessed with 21-item Depression, Anxiety, and Stress Scales (DASS-21; total possible = 42 for each sub-scale)

[c] Montreal Cognitive Assessment, normal cognition ≥ 26.

F = female, M = male.

Table 2

Linear Mixed-Effects Models Probing the Relationship Between Age Group, Arousal Condition, and Pupil Dilation on Subjective Arousal Ratings for Sound Clips

Predictors	Estimate	S.E.	Wald's 95% CI	t-value	*p*-value
Intercept	1.66	0.08	1.50, 1.82	20.46	< .001
Age	−0.06	0.08	−0.22, 0.10	−0.70	0.484
Arousal	2.16	0.029	2.10, 2.22	72.95	< .001
Pupil dilation	−20.12	64.24	−145.98, 105.74	−0.31	0.754
Age × Arousal	−0.28	0.03	−0.34, −0.23	−9.59	< .001
Age × Pupil dilation	1.95	64.24	−123.91, 127.81	0.03	0.976
Arousal × Pupil dilation	294.39	90.28	117.45, 471.35	3.26	0.001
Age × Arousal × Pupil dilation	25.36	90.28	−151.59, 202.34	0.28	0.779

Note. 95% confidence intervals were computed using confint.merMod function from the lme4 library in R. Age (1=young, −1=older), arousal (1=arousing, 0=non-arousing), and pupil dilation to sounds were modeled as fixed effects. The participant intercept was modeled as a random effect.

Table 3

Average Reaction Times (RT) in Seconds for Detecting Probes

	Young		Older	
	Arousing M (SD)	**Non-arousing M (SD)**	**Arousing M (SD)**	**Non-arousing M (SD)**
High salience body RT	.398 (.09)	.395 (.09)	.554 (.13)	.575 (.13)
Low salience body RT	.380 (.09)	.390 (.10)	.556 (.13)	.559 (.13)
High salience scene RT	.386 (.08)	.397 (.09)	.561(.14)	.571 (.15)
Low salience scene RT	.385 (.10)	.383 (.08)	.549 (.13)	.572 (.14)

Table 4

Recognition memory performance for old images

	Young		Older	
	Arousing M (SD)	**Non-arousing M (SD)**	**Arousing M (SD)**	**Non-arousing M (SD)**
High salience body image				
Hits	.24 (.15)	.22 (.14)	.21 (.12)	.20 (.14)
Gist Hits	.25 (.15)	.25 (.17)	.21 (.15)	.24 (.17)
Misses	.51 (.27)	.53 (.28)	.58 (.23)	.56 (.27)
Low salience body image				
Hits	.19 (.12)	.21 (.16)	.22 (.16)	.16 (.12)
Gist Hits	.25 (.16)	.23 (.19)	.17 (.14)	.19 (.15)
Misses	.56 (.25)	.56 (.30)	.60 (.26)	.65 (.25)
High salience scene image				
Hits	.22 (.17)	.22 (.17)	.15 (.13)	.13 (.13)
Gist Hits	.19 (.13)	.19 (.13)	.15 (.17)	.15 (.12)
Misses	.59 (.27)	.59 (.27)	.70 (.27)	.71 (.24)
Low salience scene image				
Hits	.18 (.14)	.17 (.17)	.14 (.14)	.14 (.14)
Gist Hits	.18 (.15)	.19 (.14)	.13 (.12)	.13 (.14)
Misses	.64 (.27)	.64 (.25)	.73 (.25)	.73 (.24)

Note. Hits = old image indicated as old. Gist hits = categorically similar lure indicated as old. Misses = both images indicated as new.

Table 5

Significant clusters and locations of local maxima from the whole-brain analysis of BOLD signal when viewing images during the incidental encoding task

Contrasts and activated brain regions	Cluster	*k*	Z-max	MNI coordinates x	y	z
Arousing > Non-arousing						
L Frontal orbital cortex	5	11145	6.08	−44	22	−10
L Supramarginal gyrus, posterior			6.06	−58	−44	16
L Superior temporal gyrus, posterior			6.04	−52	−36	4
L Superior temporal gyrus, posterior			5.97	−52	−40	4
L Superior temporal gyrus, posterior			5.94	−56	−40	4
L Superior temporal gyrus, posterior			5.66	−62	−34	2
R Middle temporal gyrus	4	10790	6.42	50	−38	4
R Superior temporal gyrus, anterior			6.25	62	−8	−6
R Superior temporal gyrus, posterior			6.06	64	−32	4
R Supramarginal gyrus, posterior			5.95	58	−38	8
R Superior temporal gyrus, anterior			5.94	54	0	−14
R Planum temporale			5.93	54	−22	6
R Superior frontal gyrus	3	4885	5.28	2	54	28
R Superior frontal gyrus			5.16	6	50	26
L Frontal pole			5.10	−12	58	24
L Superior frontal gyrus			5.09	−6	48	28
R Superior frontal gyrus			5.07	4	54	32
L Superior frontal gyrus			5.04	−4	52	24
R Cerebellum	2	4284	5.01	22	−74	−32
L Cerebellum			4.89	−22	−74	−36
L Occipital fusiform gyrus			4.84	22	−78	−24
L Occipital fusiform gyrus			4.66	−26	−80	−26
R Cerebellum			4.54	14	−82	−32
R Cerebellum			4.19	4	−52	−36
Cingulate gyrus, posterior	1	371	4.58	0	−40	2
R Brainstem			4.5	6	−34	0
R Brainstem			3.22	14	−22	−12
R Brainstem			2.92	12	−28	−8
High salience body > Low salience body						
R Lateral occipital cortex, inferior	2	1907	5.43	50	−74	−2
R Lateral occipital cortex, inferior			5.36	48	−80	0
R Temporal occipital fusiform cortex			5.24	44	−48	−18
R Lateral occipital cortex, inferior			5.13	48	−76	4
R Lateral occipital cortex, inferior			4.69	48	−70	−12
R Lateral occipital cortex, inferior			4.68	46	−62	−12
L Temporal occipital fusiform cortex	1	1231	5.18	−38	−46	−18

Contrasts and activated brain regions	Cluster	*k*	Z-max	MNI coordinates x	y	z
L Lateral occipital cortex, inferior			4.43	−46	−78	4
L Lateral occipital cortex, inferior			4.15	−46	−74	−10
L Inferior temporal gyrus, temporooccipital part			3.08	−50	−62	−14
L Lateral occipital cortex, inferior			2.85	−38	−80	−4
L Occipital fusiform gyrus			2.57	−38	−74	−18
High salience scene > Low salience scene						
L Temporal occipital fusiform cortex	5	994	5.67	−26	−46	−10
L Parahippocampal gyrus, posterior			5.33	−20	−38	−14
L Lingual gyrus			5.14	−28	−52	−6
L Occipital fusiform gyrus			4.48	−26	−66	−12
L Parahippocampal gyrus, anterior			3.31	−28	−20	−20
L Occipital fusiform gyrus			3.00	−22	−84	−18
R Lingual gyrus	4	664	4.92	26	−42	−10
R Lingual gyrus			4.92	26	−42	−8
R Parahippocampal gyrus, posterior			4.66	20	−36	−14
R Parahippocampal gyrus, posterior			2.64	32	−28	−2
R Lingual gyrus	3	515	3.94	16	−84	−8
R Occipital pole			3.33	12	−94	0
R Occipital pole			3.27	22	−92	4
R Occipital fusiform gyrus			2.95	26	−70	−12
R Occipital pole			2.92	20	−96	0
R Precuneus cortex	2	370	3.85	16	−54	14
R Precuneus cortex			3.37	14	−50	8
R Precuneus cortex			3.14	24	−60	20
R Precuneus cortex			2.65	10	−52	22
R Precuneus cortex			2.59	8	−50	18
R Cingulate gyrus, posterior			2.56	10	−38	0
L Lateral occipital cortex, superior	1	339	3.52	−34	−84	22
L Lateral occipital cortex, superior			3.51	−34	−88	22
L Occipital pole			3.04	−30	−90	12
L Lateral occipital cortex, superior			3.01	−28	−78	18
L Lateral occipital cortex, inferior			2.66	−30	−96	12
Young (Arousing>Non-arousing) > Older (Arousing>Non-arousing)						
R Superior frontal gyrus	4	2479	5	6	50	26
L Frontal pole			4.88	−12	42	46
L Frontal pole			4.85	−14	60	24
R Frontal pole			4.56	10	56	28
R Superior frontal gyrus			4.4	12	52	20
L Frontal pole			4.35	−20	54	24
R Temporal pole	3	1439	4.25	42	14	−38
R Temporal pole			4.22	46	20	−24

Contrasts and activated brain regions	Cluster	*k*	Z-max	MNI coordinates x	y	z
R Frontal pole			4.19	42	40	−14
R Frontal pole			4.15	40	34	−12
R Middle temporal gyrus, anterior			4.13	56	2	−22
R Temporal pole			4.09	40	20	−20
R Middle temporal gyrus, posterior	2	397	4.54	40	−32	2
R Middle temporal gyrus, posterior			4.54	40	−32	2
R Supramarginal gyrus, posterior			3.65	48	−42	10
R Middle temporal gyrus, temporooccipital part			3.17	42	−42	4
R Supramarginal gyrus, posterior			3.16	36	−40	6
R Superior temporal gyrus, posterior			2.97	56	−34	4
R Middle temporal gyrus, posterior			2.73	50	−20	−6
L Middle temporal gyrus, anterior	1	348	4.3	−50	−2	−20
L Middle temporal gyrus, anterior			4.18	−54	−6	−18
L Middle temporal gyrus, posterior			3.79	−50	−26	−6
L Middle temporal gyrus, posterior			3.72	−54	−18	−14
L Middle temporal gyrus, anterior			2.9	−58	−10	−12
L Middle temporal gyrus, anterior			2.68	−60	−4	−12
Older (Arousing>Non-arousing) > Young (Arousing>Non-arousing)						
R Superior parietal lobule	3	5782	4.33	34	−46	68
R Superior parietal lobule			4.10	32	−46	38
R Superior parietal lobule			4.03	18	−52	72
R Lateral occipital cortex, superior			4.00	30	−64	46
R Lateral occipital cortex, superior			3.97	20	−66	50
R Precuneus cortex			3.94	6	−64	62
R Superior frontal gyrus	2	801	3.92	26	0	66
R Superior frontal gyrus			3.9	26	6	58
R Superior frontal gyrus			3.78	24	20	58
R Superior frontal gyrus			3.55	20	8	48
R Superior frontal gyrus			3.37	26	10	52
R Middle frontal gyrus			3.28	32	6	62
R Middle frontal gyrus	1	395	4.06	34	36	46
R Frontal pole			3.88	36	40	42
R Middle frontal gyrus			3.67	40	34	28
R Middle frontal gyrus			3.55	36	34	26
R Middle frontal gyrus			3.54	42	34	38
R Frontal pole			3.45	46	40	30
Young (High salience>Low salience) > Older (High salience>Low salience) [a]	–		–	–	–	–
Arousing (High salience>Low salience) > Non-arousing (High salience>Low salience) [a]	–		–	–	–	–

Note. k = number of voxels; R = right; L = left.